Journal of Asian Concrete Federation
Vol. 11, No. 3, pp. 61-85, September 2025
ISSN 2465-7964/ eISSN 2465-7972
DOI http://dx.doi.org/10.18702/acf.2025.11.3.61

Review Paper

Carbon mineralization of steel slag and its application in building materials–A state–of–the–art review

Xingpei Su, Yang Yu*, Yue Wang, Xiang Hu*

(Received: 06-Aug-2025; Revised: 22-Sep-2025; Accepted: 25-Sep-2025; Published online: 30-Sep-2025)

Abstract: Steel slag is produced in large quantities annually but suffers from a low utilization rate, primarily being disposed through stockpiling or landfilling. This not only occupies land resources but also brings environmental risks due to the leaching of metal ions. Although the mineral composition of steel slag is similar to that of Portland cement, endowing it with potential as a cementitious material, it still faces challenges such as slow hydration rates, low early strength, and poor durability. Currently, mineralization of steel slag is regarded as a key strategy for achieving net-zero emissions in steel manufacture. However, reviews on cement-free mineralized steel slag compacts are still lacking. This review comprehensively outlines the research progress of mineralized steel slag, including their mineralization behaviors and characteristics, while evaluating the performance of steel slag compacts via carbon mineralization. This review is expected to provide valuable insights into the feasibility analysis of utilizing mineralized steel slag as building materials.

Keywords: Carbon mineralization; Steel slag; Low-carbon materials; Mechanical strength; Carbon emission

1. Introduction

Steel slag is the solid byproduct generated during steel-making process[1, 2]. On average, each ton of crude steel production will accompany with approximately 0.1-0.15 tons production of steel slag[3, 4]. In 2020, global steel slag production reached 180-270 million tons. However, despite its massive production, the utilization rate of steel slag remains low[5]. In China, only 22% of steel slag is effectively utilized[6, 7]. In Canada, steel slag even fails to be used in asphalt concrete[8]. In order to achieve the resource utilization of steel slag, it is crucial to select the appropriate usage scenario. The primary use of steel

*Corresponding author **Yang Yu,** *College of Civil Engineering, Hunan University, Changsha, 410082, PR China; Key Laboratory for Green & Advanced Civil Engineering Materials and Application Technologies of Hunan Province, International Innovation Center for Green & Advanced Civil Engineering Materials of Hunan Province, Changsha, 410082, PR China. E–mail: yuyang98@hnu.edu.cn*
*Corresponding author **Xiang Hu,** *College of Civil Engineering, Hunan University, Changsha, 410082, PR China; Key Laboratory for Green & Advanced Civil Engineering Materials and Application Technologies of Hunan Province, International Innovation Center for Green & Advanced Civil Engineering Materials of Hunan Province, Changsha, 410082, PR China. E–mail: xianghu@hnu.edu.cn*
Xingpei Su, *College of Civil Engineering, Hunan University, Changsha, 410082, PR China;*
Key Laboratory for Green & Advanced Civil Engineering Materials and Application Technologies of Hunan Province, International Innovation Center for Green & Advanced Civil Engineering Materials of Hunan Province, Changsha, 410082, PR China. E–mail: 471043786@hnu.edu.cn
Yue Wang, *College of Civil Engineering, Hunan University, Changsha, 410082, PR China; Key Laboratory for Green & Advanced Civil Engineering Materials and Application Technologies of Hunan Province, International Innovation Center for Green & Advanced Civil Engineering Materials of Hunan Province, Changsha, 410082, PR China. E–mail: 124264551@qq.com*

slag in comprehensive utilization is as a construction material[9, 10]. In addition, steel slag possesses the characteristics of large specific surface area, low cost, and porosity, so it can find secondary emerging uses in environment protection[10, 11], as shown in **Fig. 1**.

According to the steelmaking process, steel slag can be categorized into three types: basic oxygen furnace slag (BOFs), electric arc furnace slag (EAFs), and ladle furnace slag (LFs)[12, 13]. The mineral composition of steel slag is similar to that of Portland cement, primarily consisting of tricalcium silicate (C_3S), dicalcium silicate (C_2S), RO phases (solid solutions containing magnesium, iron, and manganese oxides), and free lime (f-CaO)[14, 15]. Considering technical feasibility, economy, and environment aspects, the utilization of steel slag as a cementitious material should be prioritized[16]. However, steel slag faces two inherent limitations during the application: Steel slag contains low content of C_3S, and high content of γ-C_2S, which exhibits poor hydraulic activity[17]. Consequently, the silicate phases in steel slag present slow hydration rates and poor early strength. Moreover, the volumes of f-CaO and free magnesium oxide (f-MgO) in steel slag will expand by 198% and 248% undergo the hydration, respectively, leading to the concrete cracking and decreasing the volume stability and durability of buildings[3, 18].

To enhance the reactivity and volume stability of steel slag, different strengthening strategies such as grinding[19], chemical activation[20], and high-temperature steam curing [21] have been proposed and utilized. However, these methods inevitably lead to additional energy consumption and environment pollution, thereby increasing the utilization cost of steel slag. It is widely known that mineral phases rich in alkaline metals such as Ca and Mg can react with CO_2 to form carbonate products[22]. This process not only mitigates the volume expansion of steel slag but also facilitates the capture and sequestration of CO_2. The resulting carbonate precipitation can further fill pores and densify the microstructure[23, 24]. Consequently, mineralization treatment of steel slag is the crucial strategy for achieving net-zero emissions in steel-making process. However, utilizing steel slag merely for carbon capture can be regarded as a wasteful use of resources[25]. In recent years, the use of cement-free steel slag compacts as building materials attracted large research attention. For example, Xian et al. demonstrated the feasibility of using steel slag as a 100% replacement for cement in concrete preparation[26]. The compressive strength of steel slag compacts achieves 50 MPa after mineralization and subsequent water curing. Humbert et al. further improved the compressive strength of steel slag bricks to 70 MPa by optimizing the moisture content and compacting pressure[27]. Ghouleh et al. activated high-strength KOBM steel slag through mineralization, and the test results revealed that the steel slag compacts exhibited a compressive strength of 80 MPa after 2 h of mineralization[28]. These studies indicate that the steel slag compacts undergoing mineralization satisfactory mechanical strength to be used as building materials and products. More importantly, Zhang et al. compared the mechanical property and carbon capture performance between full steel slag bricks and full carbide slag blocks [29]. The results showed that the maximum mineralization degree and compressive strength of steel slag blocks and carbide slag blocks were 24.56% and 79.68 MPa, and 64.46% and 44.64 MPa, respectively. This demonstrates that steel slag blocks can achieve higher mechanical performance even at lower mineralization degree. Therefore, mineralized steel slag compacts exhibit a large potential for application as building materials.

Considering these facts, we comprehensively summarize the research status of mineralized steel slag, focusing on mineralization behaviors and characteristics, and the application as building materials. This review conduces to better understanding the development of mineralized steel slag and analyzing their large-scale application prospects in the construction industry.

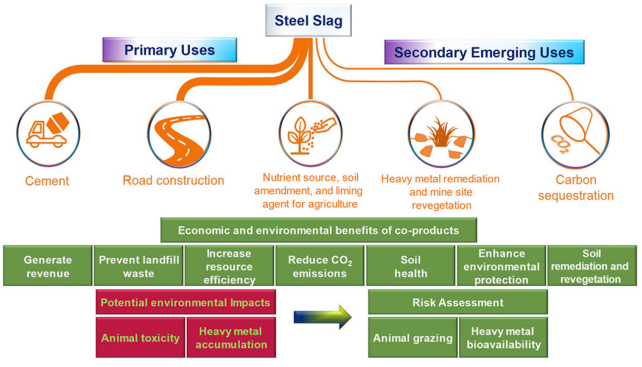

Fig. 1 Comprehensive utilization of steel slag[10].

2. Mineralization behavior of steel slag

2.1. Raw materials

As a by-product of steel production, the physical and chemical properties of steel slag depend on the raw materials and steelmaking process. According to the steelmaking process, steel slag can be divided into three categories: BOF, EAF, and LF slag[13]. BOF slag and EAF slag are both produced during the first refinement of steel and the major difference between them is the heating strategy. BOF slag uses the pure oxygen to initiate the oxidation reaction at around 1600 ℃. Hence, the main components of BOF slag are calcium, iron and silicon oxides. EAF slag possesses similar composition to BOF slag because they have the similar production process. But unlike BOF slag uses the gaseous fuels, the EAF uses electric arc transformer connected three graphite electrodes to heat the steel. LF slag is produced during the second refinement of the molten steel from the BOF and EAF. And the LF uses the same heating method as EAF.

The chemical composition of steel slag is very complex, mainly including CaO, SiO_2, Fe_2O_3/FeO, MgO and Al_2O_3. However, the contents of CaO and Fe_2O_3 in the BOF slag are approximately 40–50 % and 20–30 %, respectively[3]. For EAF slag, the CaO and FeO occupy the large proportion, the CaO content ranges from 22% to 60% and the FeO content can go up to 40%[30]. In terms of LF slag, the CaO is also the major composition, accounting for 42%-57%. The SiO2 content can reach about 20% and the FeO content is less than 5%[31]. Moreover, it is worth noting that the chemical composition of steel slag not only depends on the steelmaking process, but also is affected by the diversity of raw materials, such as the recycled steel scraps, pig iron. Therefore, the chemical composition of steel slag is extremely complex, which consequently leads to significant variability in its mineralization reactivity.

2.2. Mineralization reaction

Steel slag exhibits remarkably high mineralization activity. When exposed to CO_2 environment, f-CaO, f-MgO, and calcium silicates are mineralized, generating $CaCO_3$ precipitates and silica gels. Additionally, Fe and Mn within the RO phase can also be mineralized and translated to mineralization products. These mineralization products interweave and fill to create a stable and dense microstructure, endowing steel slag compacts with large mechanical strength[32]. C_2S is the main component of calcium silicate in steel slag. C_2S possesses four well-established polymorphs：α, α', β and γ. When C_2S is cooled from high temperature, α-C_2S converts into β-C_2S at 630 ℃, and then transforms to γ-C_2S at lower temperature[33]. Therefore, C_2S in steel slag mainly exists in the form of γ-C_2S. Bukowski et al. pointed out that γ-C_2S with poor hydraulic property exhibited higher mineralization activity than β-C_2S. The compressive strength of mortar compacts with γ-C_2S could reach 50 MPa underwent the mineralization in 1 MPa CO_2 for 15 min[34]. According to the study by Mo et al., 100% steel slag compacts generated 34.3% $CaCO_3$ after 14 d mineralization. This resulted in a reduction of pore size from 0.2-3 μm before mineralization to 0.1-1 μm after mineralization, ultimately making the compressive strength of full steel slag compacts reach 44.1 MPa[35]. However, according to the works of Shao et al., the compressive strength of steel slag compacts was only 2-4 MPa after 12 h of hydration [36]. These studies above indicate that mineralization is the main contribution to the mechanical properties of steel slag compacts.

The mineralization process of steel slag is mainly divided into two strategies: wet mineralization and dry mineralization. In terms of dry mineralization, CO_2 primarily diffuses into the interior of steel slag, directly reacting with solid mineral phases to form $CaCO_3$ precipitate and silica gel. Generally, the water-binder ratio (w/b) of steel slag compact prepared by dry mineralization is less than 0.2. The main reaction process is as follows：

$$2(2CaO{\cdot}SiO_2)+CO_2+3H_2O \rightarrow 3CaO{\cdot}2SiO_2{\cdot}3H_2O+CaCO_3 \quad (1)$$

$$2(3CaO{\cdot}SiO_2)+3CO_2+3H_2O \rightarrow 3CaO{\cdot}2SiO_2{\cdot}3H_2O+3CaCO_3 \quad (2)$$

$$CaO+CO_2 \rightarrow CaCO_3 \quad (3)$$

$$MgO+CO_2 \rightarrow MgCO_3 \quad (4)$$

Wet mineralization involves gas-liquid-solid multiphase interactions[37], including: 1) CO_2 dissolves

in the liquid phase to form carbonic acid (H_2CO_3), which then ionizes to produce H^+ and CO_3^{2-}; 2) calcium and magnesium dissolve and diffuse into the liquid phase, forming Ca^{2+}/Mg^{2+};3) Ca^{2+}/Mg^{2+} reacts with CO_3^{2-} to generate $CaCO_3$/ $MgCO_3$, which precipitates on the surface of steel slag or within the liquid phase. Fig. 2 illustrates the wet mineralization process of minerals occurring at solid, liquid, and gaseous three-phase interfaces[38]. And the main processes are as follows:

$$CO_{2(g)} \leftrightharpoons CO_{2(aq)} + H_2O_{(l)} \leftrightharpoons HCO_{3(aq)} + H^+_{(aq)} \leftrightharpoons CO^{2}_{3(aq)} + 2H^+ \quad (5)$$

$$(Ca/Mg)SiO_{3(s)} + 2H^+_{(aq)} \rightarrow (Ca^{2+}/Mg^{2+})_{(aq)} + SiO_{2(s)} + H_2O_{(l)} \quad (6)$$

$$(Ca^{2+}/Mg^{2+})_{(aq)} + CO^{2}_{3(aq)} \rightarrow (Ca/Mg)CO_{3(s)} \quad (7)$$

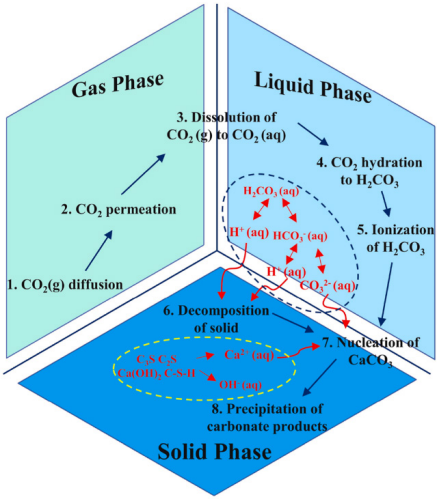

Fig. 2 Mineralization process at three-phase interfaces[38].

Dry mineralization is the simplest and most direct mineralization method, providing lower energy consumption compared to wet mineralization[39]. Since the use of steel slag compacts as building materials requires large-scale and low-cost production, dry mineralization is more suitable for the practical application scenarios of steel slag compacts [40]. This also explains why the majority of existing studies on steel slag compacts choose dry mineralization.

2.3. Liquid phase change of wet mineralization

Wet mineralization is accompanied by changes in solution pH and ion concentration, particularly the Ca^{2+} concentration and CO_2 dissolution rate, which significantly influence the mineralization rate and degree.

2.3.1. pH change

The dissolution of calcium-bearing minerals in steel slag releases Ca^{2+} and OH^-, resulting in an alkaline solution (initial pH ~12.7) at the onset of mineralization. Compared to other calcium-based minerals, $Ca(OH)_2$ exhibits higher solubility and dissolution. Consequently, Chang et al. concluded that the OH^- in the liquid phase during wet mineralization predominantly originated from $Ca(OH)_2$ dissolution[41]. In their study, the solution pH remains virtually constant during the initial mineralization stage (within 10 min), while a rapid decline in $Ca(OH)_2$ content is observed (Fig. 3). For steel slags with low $Ca(OH)_2$ content, the initial alkalinity of the solution

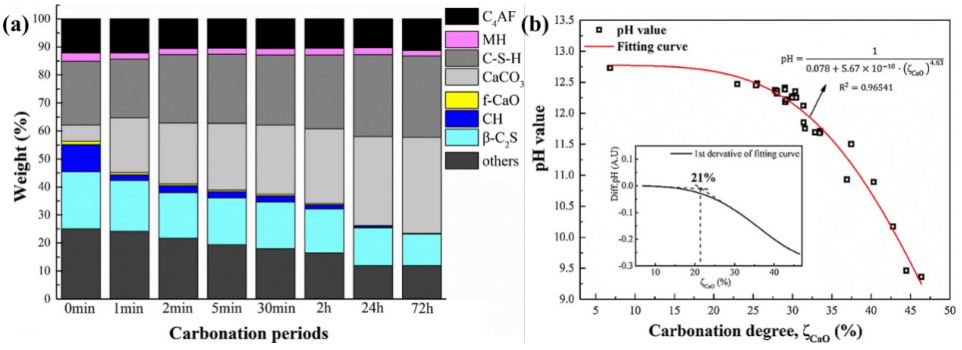

Fig. 3 (a) Mineral components of mineralized steel slag; (b) pH change during mineralization[41].

is primarily governed by the dissolution of C_2S, C_3S, and f-CaO. In the study by Li et al., the steel slag used contained negligible $Ca(OH)_2$. The initial solution pH shows a slight decrease with increasing temperature but remains consistently within the range of 12.0–12.5[42]. For steel slags with low $Ca(OH)_2$ content, the initial pH plateau phase may not be clearly observed. In addition, the wet mineralization exhibits rapid reaction kinetic, with the pH showing a fast decline throughout the reaction. The mineralization reaction is considered to reach its maximum extent when the pH stabilizes around 6.5.

2.3.2. Ions concentration change

During the dissolution of steel slag, the leaching rate of Ca is significantly higher than that of other elements such as Fe, Al, and Mn. This is related to their contents and chemical forms in the steel slag. According to the study of Lekakh et al., initially, calcium-containing minerals on particle surface dissolve rapidly, releasing Ca^{2+}. Subsequently, the remaining insoluble minerals on the surface inhibit the dissolution of internal minerals, resulting in a two-stage Ca leaching pattern featuring an initial fast phase followed by a slower phase[43]. Chang et al. demonstrated that the Ca concentration remains relatively high during the initial mineralization stage[41]. Subsequently, the calcium carbonate layer formed on the steel slag surface inhibits Ca leaching, leading to a rapid decrease in Ca concentration. Upon reaching the mineralization limit, the Ca concentration stabilizes at a relatively low level. Si is predominantly leached from C_2S, with its concentration increasing as mineralization progresses. This indicates that amorphous silica gel formed during mineralization dissolves and releases additional Si.

Carbon mineralization decreases pH, consequently resulting in concentration changes of CO_3^{2-} and HCO_3^- in solution, as illustrated in Fig. 4[44]. When the pH is below 4, CO_2 predominantly exists in the form of H_2CO_3. Within the pH range of 4-8, H_2CO_3 undergoes dissociation, releasing HCO_3^- ions. When the pH ranges between 8 and 12, HCO_3^- undergoes further dissociation to release CO_3^{2-} ions, with the concentration of CO_3^{2-} increasing as pH rises. When pH exceeds 12, CO_3^{2-} becomes predominant in the system.

2.4. CO_2 diffusion and ions leaching of dry mineralization

Compared to the wet mineralization, the dry

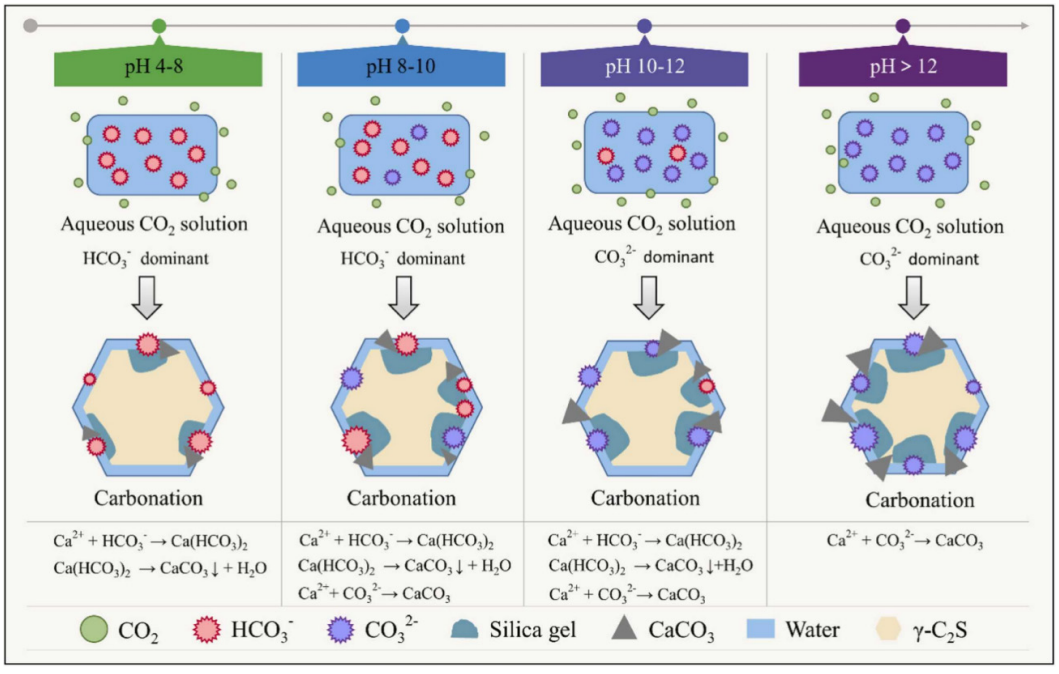

Fig. 4 Carbon mineralization in various pH ranges[44].

mineralization requires consideration of CO_2 diffusion behavior within steel slag particles or compacts. CO_2 diffuses primarily through pores. Increasing pore water content enhances Ca leaching and CO_2 diffusion. However, excessive water content also inhibits CO_2 diffusion. Lin et al. disclosed that increasing the water content from 6% to 7% significantly raised the proportion of closed pores (from 0.79% to 3.46%) [45]. A further increase to 8% water content elevated the closed pore ratio to 5.09%. Fig. 5 illustrates the impact of water content on pore structure. Increasing water content enhances the formation of bridging water between particles, where calcium carbonate precipitation occurs. This process significantly increases the proportion of closed pores, consequently impeding CO_2 diffusion. In addition, raising the temperature increases the average kinetic energy of gas molecules, thereby accelerating the CO_2 diffusion rate and improving the mineralization degree[46]. Furthermore, according to Fick's first law, the diffusion rate is directly proportional to the concentration gradient. Hence, increasing CO_2 concentration strengthens the diffusion driving force, thereby promoting its transport in solution. As described by Henry's law, elevating CO_2 pressure significantly improves its solubility, consequently increasing the concentration gradient. Therefore, appropriately increasing both CO_2 concentration and pressure is conducive to improving mineralization efficiency in steel slag[47, 48].

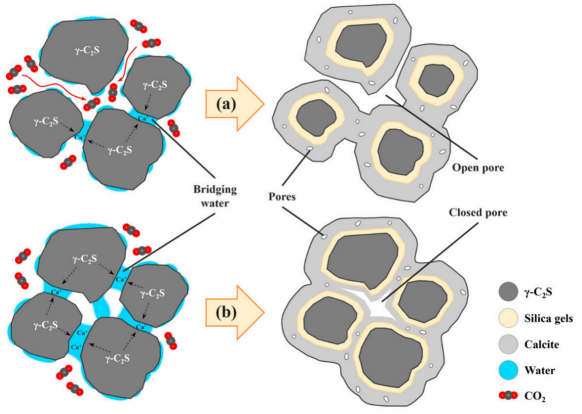

Fig. 5 Pore structure of carbon mineralized steel slag under various water content: (a) Water content < 7%; (b) Water content > 7%[45].

In dry mineralization process, the relatively slow reaction results in small pH variation of mineralized steel slag leachates. Spanka et al. investigated pH evolution during dry mineralization of three steel slags[49]. At a water-to-solid ratio of 2, all steel slag eluates exhibit initial pH values no lower than 11. After reaching the mineralization limit, the pH remains above 9. This may be attributed to the decreased water content and increased closed pores, which hinder CO_2 diffusion and dissolution in the later stage of mineralization. Librandi et al. systematically analyzed the ion concentrations of mineralized steel slag leachates[50]. Their results reveal that the Ca^{2+} concentration decreases with the extended mineralization time. Upon reaching the mineralization limit, the Ca^{2+} concentration stabilizes at a relatively low level (100 mg/L) and remains constant. This demonstrates that upon reaching the mineralization limit, Ca^{2+} fails to react and participate. In addition, the mineralization limit is not governed by the Ca^{2+} concentration in the pore solution. The leaching of Mg is primarily governed by the magnesium-bearing phases in steel slag, such as $Ca_3Mg(SiO_4)_2$ and $Ca_7Mg(SiO_4)_4$. As calcium silicates and portlandite dissolve, these Mg^- containing minerals become exposed to aqueous. The gradual increase of Mg^{2+} concentration observed during mineralization indirectly indicates that the participation degree of Mg^{2+} in carbon mineralization is very low.

3. Characteristics of mineralized steel slag

3.1. Mineralization models

The most well-known models for the mineralization of steel slag are shrinking core model and surface coverage model. Both models assume that the particles are uniform spheres. As illustrated in Fig. 6a, the mineralization process of steel slag particles in the shrinking core model primarily involves the diffusion of CO_2 through the mineralized product layer and chemical reaction between CO_2 and unreacted core. As the mineralization reaction progresses, a multi-layered structure forms comprising an outer layer of $CaCO_3$, an intermediate layer of silica gel, and an inner layer of unreacted core. Geng et al. utilized a 3D X-ray microscope system to analyze the 3D structure of

mineralized steel slag particles, revealing a high degree of consistency with shrinking core model[40]. The specific 3D model and structure of individual steel slag particle are shown in Fig. 6b. In shrinking core model, mineralization reaction occurs on the entire surface of the unmineralized core. The reaction process can be described by the classical kinetic equation:

$$\left[1-(1-\alpha)^{1/3}\right]^{n} = kt \quad (8)$$

Where α represents the degree of mineralization. k and t are the apparent reaction rate constant and the reaction time. The value of n is normally equal to 1 or 2, which indicates the rate-determining step is interface chemical reaction controlled or diffusion controlled through the mineralization product layer, respectively.

Based on the shrinking core model and Eq. (8), both Tu et al. and Kim et al. used two n values (1 and 2) to fit the mineralization of steel slag, respectively[51, 52]. Their fit results are consistent that the R^2 value of "n=2" is higher than that of "n=1", indicating that the rate-determining step of steel slag mineralization is CO_2 diffusion through mineralization product layer (Fig.6d). In addition, according to the kinetic study by Tu et al., the diffusion rate of CO_2 through the mineralized layer was closely related to the mineralization temperature. Other parameters exhibited negligible influence on the diffusion rate[51, 53]. Kim et al. utilizing shrinking core model proved that the thickness of the outer layer ($CaCO_3$ layer) on steel slag particles remains consistent at 5.2 ± 1.6 μm, regardless of the particle size[52] (Fig.6c). However, Wang et al. pointed out that the rate-limiting step during initial stage was likely to be the interface chemical reaction because the product layer was thin in this stage[54]. There was a transition point between the two rate-limiting steps. As shown in Fig.6e, the piecewise fitting possesses better effect than the fitting result by single n value, suggesting that rate-limiting step will change from interface chemical reaction to CO_2 diffusion. In addition, the smaller the steel slag size, the later the transition point. This is attributed to the fact that reducing particle size increases the specific surface area of steel slag, thereby delaying the coverage of surface by the product layer. Recently, in the review of DiGiovanni et al.,

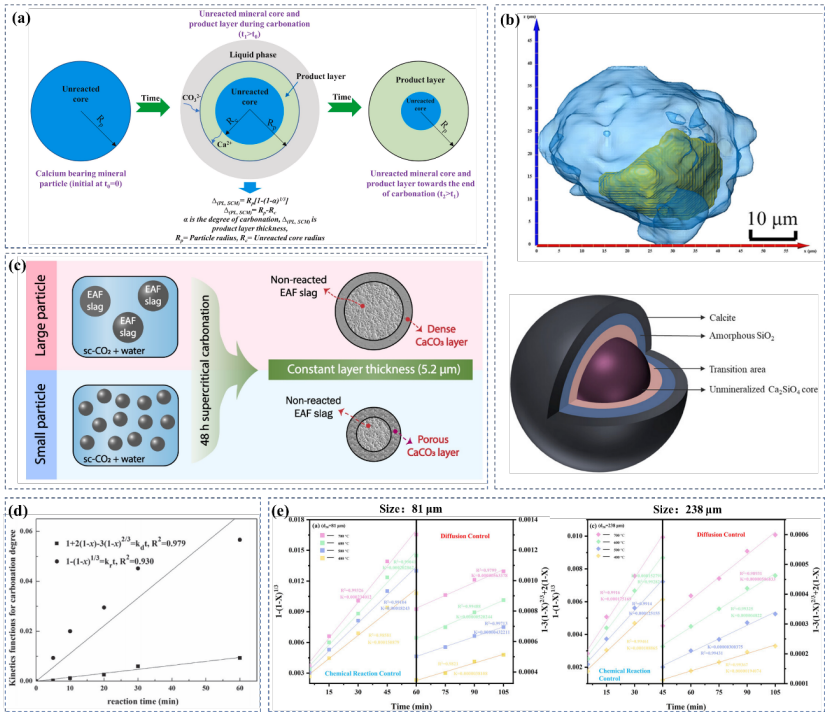

Fig. 6 (a) Schematic diagram of shrinking core model[38]; (b) 3D structure and model of mineralized steel slag particle[40]; (c) Mineralization of steel slag particles with various sizes[52]; (d) Mineralization degree versus reaction time fitted by two n values[51]; (e) Piecewise fitting results with diverse sizes[54].

they pointed out that the shrinking core model could be used to accurately describe the process that as the mineralization product layer grows, the diffusion distance increases, thereby slowing the mineralization reaction[53]. Considering the fact above, the shrinking core model possesses significant value for investigating the mineralization efficiency and rate-determining factors of individual steel slag particles.

In addition to the shrinking core model, the surface coverage model proposed by Ho and Shih has been proven highly effective in describing the mineralization process of alkaline aluminosilicate minerals[55]. Unlike the shrinking core model, the surface coverage model assumes that the mineralization reaction only takes place on the reactive surface not covered by the product layer. The schematic diagram is illustrated in Fig. 7a. In this model, the mineralization degree reaches maximum when the particle surface is completely enveloped by the mineralization products. The surface coverage model can be briefly expressed by the following equations[56]:

$$\frac{d\delta_{Cao}}{dt} = S_g M \cdot r_s = S_g M \cdot k_s \Phi \tag{9}$$

$$-\frac{d\Phi}{dt} = k_p \Phi^{n-1} \cdot r_s = k_p \cdot k_s \Phi^n \tag{10}$$

$$k_1 = k_s S_g M \tag{11}$$

$$k_2 = k_p/(S_g M) \tag{12}$$

Where the and are the rate of mineralization and the fraction of active surface sites. Sg (m^2/g), rs (mole/min/m^2), ks, and kp represent the initial specific surface area, mineralization reaction rate per initial surface area, the rate constant, and the proportional constant.

Zhang et al. applied the surface coverage model to fit the mineralization degree of three types of steel slag, achieving R^2 values greater than 0.98, indicating excellent agreement between the mineralization kinetics of steel slag and shrinking core model [57]. The fitting results are shown in Fig.7b. According to their studies, the initial mineralization process was primarily limited by the precipitation of mineralization products. As the reaction progresses, the dissolution of minerals at uncovered reactive sites became the dominant factor controlling the reaction rate. This differs from the shrinking core model that the reaction rate at later stages is controlled by CO_2 diffusion. Wang et al. pointed out that the previous work of shrinking core model was focused on the loosely-connected particles either covered a thin moisture layer or immersed in suspension, like the mineralization of steel slag particles[58]. When applying this model to investigate the mineralization behavior of γ-C_2S compacts at different temperatures, only the case of 0 °C yields an n value close to 2. In contrast, the n values at other temperatures fall in the range of 3–5, significantly higher than the theoretical value of 2, as shown in Fig. 7c. However, when using the surface coverage model, the value of n is 1.7. And both experimentally-obtained and simulated conversion α at different temperatures can achieve a good fit, as shown in Fig. 7d. Due to the consideration of moisture effect, surface coverage model is more suitable to investigate the reaction kinetics of bulk samples prepared by compacting wet particles under pressure[58]. More importantly, since most steel slag products are prepared through compacting method, the surface coverage model may possess greater potential than shrinking core model for investigating the mineralization of steel slag products.

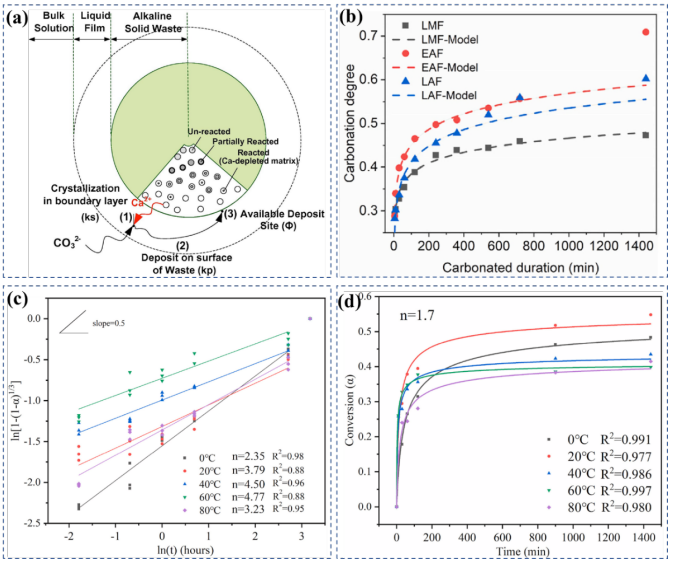

Fig.7 (a) Schematic diagram of surface coverage model[56]; (b) Model fitting results of mineralization degree[57]; (c) versus ln(t) at different temperatures and (d) The fitting results at different curing temperatures (n =1.7)[58].

3.2. Microstructure

$CaCO_3$ formed during steel slag mineralization progressively fills pores, leading to microstructural densification. Chang et al. demonstrated that carbon mineralization significantly altered the pore structure of steel slag compacts, reducing the most probable aperture from 0.734-2.517 μm to 0.016-0.047 μm. Furthermore, pores larger than 50 μm are obviously reduced[59]. Due to the lower energy required for heterogeneous nucleation of $CaCO_3$ compared to homogeneous nucleation in solution, $CaCO_3$ preferentially nucleates and grows on steel slag surfaces, forming a dense product layer. Yadav et al. directly observed through electron microscopy that $CaCO_3$ primarily grew on steel slag surfaces, with only a minimal quantity of $CaCO_3$ crystals dispersed in the solution[60]. Mo et al. discovered the clear layers from exterior to interior of mineralized steel slag: $CaCO_3$ layer, silicon-rich layer, and unreacted core layer[35], as illustrated in Fig. 8a-b. Wang et al. analyzed the distribution of RO phases after mineralization and found that these phases were encapsulated within iron-rich layers [61]. Due to the low solubility of iron-bearing phases, the RO phases fail to be mineralized, as demonstrated in Fig. 8c. In addition, due to the formation of silica gel and C-S-H, the specific surface area of steel slag increases with the improvement of mineralization degree. According to the results of Fang et al., the specific surface area of steel slag increased from 7.13m^2/g to 7.84m^2/g after 10 min mineralization and to 12.67m^2/g after 120min mineralization[62].

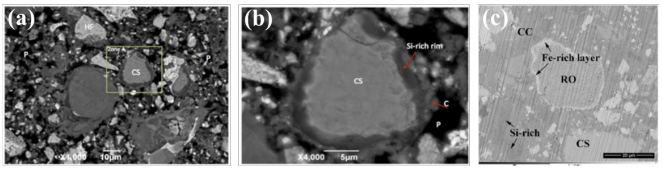

Fig.8 BSE images of mineralized steel slag; (b) is closer look at zone A in(a) [35]; (c) RO phase[61]

3.3. Composition and Polymorph control

The primary mineralization products of steel slag are $CaCO_3$ and amorphous silica gel. Zhang et al. investigated the phase composition evolution of three steel slags during wet mineralization[57], as illustrated in Fig. 9. The results show that the contents of gehlenite and FeO remain constant during mineralization, whereas mayenite, C_2S, and MgO exhibit reduced tendency. Liu et al. unveiled the phase change of steel slag under various temperature and CO_2 pressure[63]. The results demonstrate that magnesioferrite, srebrodolskite, and FeO exhibit negligible participation in mineralization even under elevated temperature and pressure condition. $Ca(OH)_2$ demonstrates remarkably high mineralization reactivity, achieving up to 80% mineralization degree without elevated temperatures or pressures. In addition, due to the hydration reactivity of steel slag, the wet mineralization must consider the synergistic effects between mineralization and hydration on mineral phase transformations. For instance, under high water-to-solid ratios, the hydration of f-MgO and f-CaO may lead to increased formation of highly mineralization-reactive $Ca(OH)_2$ and $Mg(OH)_2$ phases.

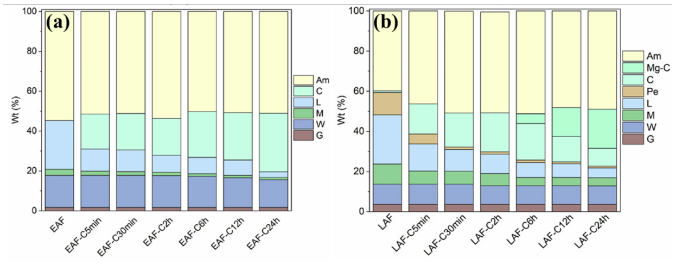

Fig.9 Mineral components of different types of steel slag: (a) EAFs; (b) LAF slag (L: Larnite; W: Wuestite; G: Gehlenite; M: Mayenite; B: Brucite; P:$Ca(OH)_2$; Pe: MgO; C: $CaCO_3$; Mg-C: Magnesium Calcite; Pe: Periclase; Am: Amorphous)[57].

$CaCO_3$, primarily in the form of calcite, aragonite, and vaterite, constitutes the dominant mineralization product[64]. Among these polymorphs, vaterite and aragonite are thermodynamically metastable and tend to spontaneously transform into calcite. Consequently, calcite predominates as the final product in conventional steel slag mineralization systems. Recent studies have revealed that specific additives could promote the formation and stabilization of metastable $CaCO_3$ phases, thereby controlling the crystallization of $CaCO_3$. The controlled crystallization of aragonite primarily utilizes magnesium-containing compounds

such as $MgCl_2$, $MgSO_4$, and $Mg(OH)_2$. Studies reveal that magnesium ions in solution partially substitute calcium ions in $CaCO_3$[65], as illustrated in Fig. 10a. This substitution preferentially occurs in calcite, where the resulting Mg-doped calcite exhibits reduced structural stability, thereby effectively suppressing the aragonite-to-calcite phase transformation. Wang et al. demonstrated that moderately increasing $MgCl_2$ concentration enhanced both the proportion and aspect ratio of aragonite[66]. However, at excessively high magnesium concentrations, partial incorporation of magnesium ions into the aragonite lattice induced structural distortion, thus inhibiting the crystal growth of aragonite. In addition, Williams et al. discovered that introducing chemically synthesized aragonite as crystal seeds during mineralization not only ensured the stability of the original seeds but also induced the formation of new aragonite crystals[67], as illustrated in Fig. 10b. Both Zhou and Ding observed consistent results: when subjecting aragonite-containing samples to secondary mineralization, the products contained higher aragonite content compared to control groups[68, 69].

In addition to vaterite, ammonium-based compounds and amino acids exhibit stabilizing effects on vaterite. Like NH_4Cl, it not only regulates the solution pH to a range more favorable for vaterite formation and stabilization, but the ammonium ions (NH_4^+) also preferentially adsorb onto specific crystal facets of vaterite, thereby inhibiting its polymorphic transformation. As for acidic amino acids, they will ionize hydrogen ions, and the remaining negatively charged groups will bind with calcium in $CaCO_3$. This interaction alters the thermodynamic properties of vaterite, consequently enhancing its stability[70], as illustrated in Fig. 10c. Song et al. investigated the effects of three ammonium salts at varying concentrations on vaterite formation and stabilization during carbide slag mineralization[71]. Their results demonstrates that within an optimal concentration, all three salts enable vaterite to account for over 90% of $CaCO_3$ product. Zhou et al. reported that when the molar ratio of glycine to Ca^{2+} reached 3:1, vaterite accounted for 99.1% of the total $CaCO_3$ produced during carbide slag mineralization[72]. However, the aforementioned additives exhibit limited effectiveness in steel slag systems. Cao et al. observed that adding glycine at varying concentrations during steel slag mineralization produced only calcite as the final product[73]. Compared to carbide slag, steel slag possesses more complex mineralogical composition, suggesting that other factors in mineralization may attenuate the efficacy of these additives.

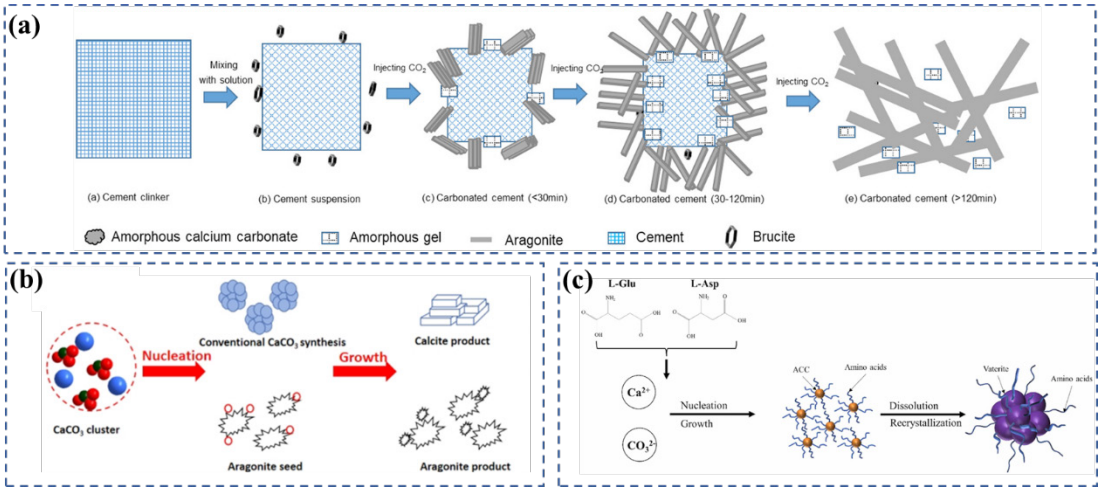

Fig.10 (a) Induce effect of aragonite seed[65]; (b) Polymorph control of magnesium ions[67]; (c) Stabilization mechanism of vaterite under the action of amino acids[70].

4. Characteristics of steel slag compacts via carbon mineralization

4.1. Performance of steel slag compacts

4.1.1. Mechanical strength

Mechanical strength is the fundamental property of mineralized steel slag compacts as construction material. Steel slag exhibits poor hydration activity. Thus, the mechanical strength of mineralized steel slag compacts is mainly derived from the mineralization. Xian et al. prepared wet-cast 100% steel slag concrete and investigated its strength development[26]. The ambient-pressure mineralization increased the compressive strength from 2.3 MPa to 38.5 MPa. It is worth noting that the compressive strength continued to increase by 9.1 MPa after a subsequent 27-day water curing. Ultimately, steel slag concrete possesses the comparable compressive strength to Portland cement concrete. Moreover, Humbert et al. enhanced the compressive strength of mineralized steel slag compacts to over 70 MPa by optimizing mineralization conditions, including temperature, compacting pressure, and CO_2 pressure[27]. In addition, Ghouleh et al. reported that the compressive strength of fully high-strength steel slag compacts achieved 80 MPa underwent 2 h mineralization[28]. Similar to the findings of Xian et al., subsequent water curing after mineralization can further enhance the mechanical properties of steel slag compacts. In conclusion, the mechanical strength of mineralized pure steel slag compacts exhibits sufficient availability for practical engineering.

4.1.2. Volume stability

Volume stability is an important index to evaluate the durability of building materials. After calcination at high temperature, many f-CaO and f-MgO will be generated in steel slag. They will cause the volume expansion undergo the hydration reaction, resulting in the structural damage of buildings. Specifically, hydration of f-CaO and f-MgO produces $Ca(OH)_2$ and $Mg(OH)_2$, leading to the volume expansion by 198% and 248%, respectively. This is one of the main challenges hindering the large-scale direct application of steel slag compacts in construction materials. The previous studies proved that mineralization could significantly eliminate the volume expansion of steel slag. For example, Fang et al. reported that the volume of cement blocks showed negligible expansion when the mineralized steel slag as SCMs replaced 30% cement [62]. The detail is shown in Fig. 11a. The result complies the requirement for Portland cement outlined in GB/T 750–92. DTG results indicate that the content of $Ca(OH)_2$ and $Mg(OH)_2$ are obviously reduced, suggesting that mineralization can effectively react f-CaO and f-MgO and control the expansion of steel slag. Mo et al. prepared prismatic concrete used steel slag even replaced 60% cement, and underwent 14 d mineralization, subsequently[74]. The prismatic concrete after mineralization presents excellent volume stability with little deterioration (Fig. 11b) and the expansion curve of concrete drops significantly (Fig. 11c). Hence, even though processing into product form may reduce the mineralization efficiency of steel slag, the volume stability of steel slag products can still be controlled through mineralization.

So far, to the best of our knowledge, there is limited research about the volume stability of full steel slag compacts. Hou et al. reported that bricks prepared by full steel slag as binder after 30 min mineralization presented no fracture[75]. Similarly, according to the results of Pang et al., f-CaO content was greatly reduced from 6.2% to less than 1% and the expansion ratio of full steel slag bricks was 0% after expansion treatment (autoclave and immersion)[76] (Fig. 11d). Wang et al. also pointed out that when the content of f-CaO was within 2.09%, steel slag presented satisfactory stability over 4 years[77]. Hence, the researches above suggest that even for full steel slag compacts, mineralization can still endow them with satisfied volume stability.

In addition, it is worth noting that although the volume of $CaCO_3$ is 12% larger than that of $Ca(OH)_2$, this does not lead to the volume expansion. The two main reasons are as follows: 1) Due to the high porosity of steel slag bricks, the volume of $CaCO_3$ generated during mineralization is much lower than the pore volume of the original bricks; 2) CO_2 is dissolved in the pore solution and then reacts with Ca^{2+} to form $CaCO_3$. In this process, $CaCO_3$ mainly precipitates and grows in

the voids. Therefore, mineralization not only prevents the volume expansion of steel slag bricks, but also fills the pores, reduces the porosity, and improves the density of the microstructure. The changes of porosity and $CaCO_3$ volume are shown in Fig. 11e.

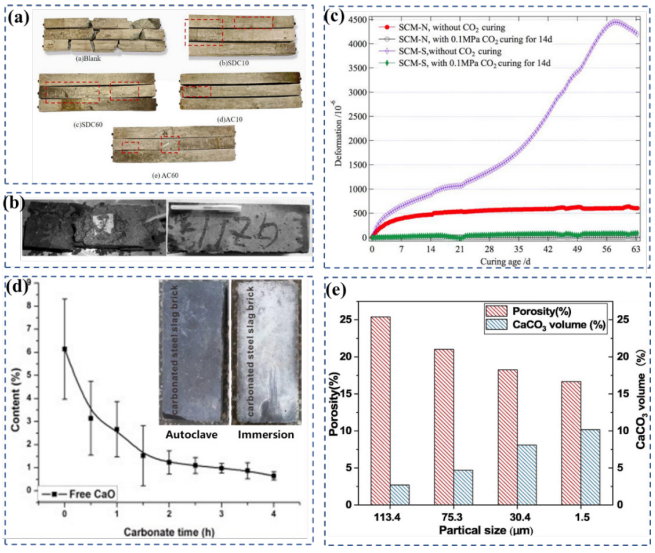

Fig. 11 (a) Autoclave expansion performance of mineralized steel slag bricks[62]; (b-c) Optical images and expansion curves of concrete prisms with/without mineralization[74]; (d) Change of f-CaO content (photos of steel slag bricks after autoclave and immersion, inset)[76]; (e) Relationship between the porosity of the brick and the volume of $CaCO_3$[75].

4.1.3. Freeze–thaw resistance

Freeze-thaw resistance also is a crucial evaluation index of construction bricks, especially in plateau region. According to the work of Hou et al., the compressive strength of mineralized steel slag bricks decreased by 20% and the mass loss was 3.2% after 50 freeze-thaw cycles, respectively. Their freezing resistance level reaches F50 [75]. The satisfied freeze-thaw resistance of steel slag bricks is attributed to the fact that water is the key to freeze-thaw destruction, and the water content in steel slag bricks is much lower than that of cement concrete. Mahoutian et al. prepared cement-free steel slag bricks using mineralization technology and compared the freeze-thaw resistance with commercial cement bricks[78]. According to their results, commercial bricks and steel slag bricks start losing mass after 2 and 7 cycles, separately. After 20 cycles, the mass of commercial cement bricks reduces by 32%, while that of steel slag bricks only reduces by 17%. Obviously, steel slag bricks present higher resistance of freeze-thaw. Moreover, Xian et al. prepared cement-free steel slag slabs and compared the resistance of freeze-thaw between carbon mineralization and ambient curing samples[79]. The results show that mineralization significantly enhances the resistance to freeze-thaw deterioration of steel slag slab. This is attributed to the fact that the generation and precipitation of $CaCO_3$ densify the microstructure and decrease the permeability. In conclusion, steel slag compacts possess excellent freeze-thaw resistance mainly due to two reasons: 1) the lower w/b through dry-cast method; 2) the denser microstructure and lower permeability benefit from mineralization.

Considering the stronger freeze-thaw resistance, the usage scenario of steel slag compacts has been further broadened. In some plateau region or cold region, steel slag compacts exhibit larger application potential compared to the commercial cement products.

4.1.4. Carbon emission evaluation

In addition to the resource utilization of steel slag, another expectation of using mineralized steel slag compacts is to achieve net-zero emissions in the construction industry. The global warming potential (GWP) is selected as the main indicator to quantify the environment impact of using mineralized steel slag products. Zhang et al. reported that the GWP of 1 m^3 mineralized steel slag compacts was in the range of 39.2 to 247.5 kg CO_2-eq, which was much lower than 1204.4 kg CO_2-eq of conventional cured OPC[80]. When the raw material production is not considered, the GWP distribution is shown in Fig. 12a. In addition, when the mineralization uses the hot flue gas released from stacks, the GWP can be further reduced by 45%. Xian et al. also illustrated that due to the elimination of cement usage and energy-intensive curing methods, mineralized steel slag products exhibit significantly lower GWP, energy consumption, and total cost[26] (Fig. 12b). Moreover, the previous studies also directly calculated the net CO_2 emission of mineralized steel slag products. In the study of biochar-modified

mineralized steel slag products, when the steel slag replacement ratio was 70%, the lowest net CO_2 emission achieved −39.9 kg/ton[9]. Ghouleh disclosed that the cumulative carbon footprint of a single steel slag block was 2.25 kg CO_2. Each block could capture 2.93 kg CO_2. Therefore, the net-CO_2 emission for a steel slag block was −0.68 kg[81]. According to the study of Mahoutian, the steel slag block production plant could be set up next to steel factory, therefore, the cost and energy consumption for transportation were negligible[78]. Their analysis indicates that the production of one steel slag block can result in 0.23 kg reduction of CO_2 from atmosphere. In contrast, the production of one commercial cement block emits 1.56 kg CO_2. Consequently, the carbon-negative characteristic endows mineralized steel slag products with larger and viable application prospects.

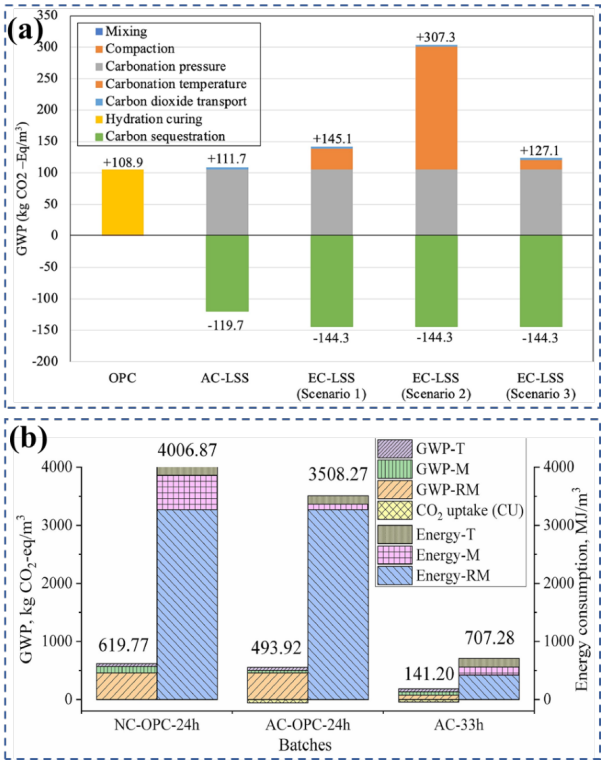

Fig. 12 (a) The GWP distribution of mineralized steel slag products and OPC concrete[80]; (b) The GWP distribution and energy consumption of mineralized OPC and mineralized steel slag products[26].

4.2. Enhancement strategies of steel slag compacts

4.2.1. Optimize mineralization condition

The mineralization conditions of steel slag compacts, including temperature, CO_2 pressure, compacting pressure, and moisture content, are closely related to the mineralization degree. A comprehensive understanding of the influence of mineralization conditions on steel slag compacts is essential for achieving optimal properties through the most cost-effective production in practical application.

Temperature is considered one of the key variables influencing the mineralization efficiency[82, 83]. Numerous studies demonstrate that appropriately increasing the mineralization temperature can effectively accelerate the mineralization of steel slag powder[84]. However, Luo et al. pointed out that when steel slag was used on a large scale as building material, steel slag was usually pressed into compacts with a low w/b, and the CO_2 pressure was relatively low during the mineralization process. In this case, whether increasing the mineralization temperature is beneficial for the mineralization development of steel slag compacts remains unclear[46]. According to the study by Zhang et al., the compressive strength of steel slag compacts mineralized at 55 °C (74.7 MPa) was 33% higher than that at 23 °C (56.1 MPa). However, when the temperature further increased to 70 °C, both CO_2 absorption and compressive strength decreased[80]. The strength change with temperature is shown in Fig. 13a. Two explanations have been proposed for this phenomenon: one is that excessively high temperature limits the dissolution of CO_2, thereby reducing the availability of CO_3^{2-}; the other is that excessively high temperature causes rapid evaporation of moisture from the steel slag compacts, leading to insufficient water for mineralization.

Zhong et al. pointed out that temperature and CO_2 pressure were two crucial factors affecting mineralization process[85]. According to their results, the optimal CO_2 pressure is 0.55 MPa. When the CO_2 pressure exceeds this threshold, although increasing pressure is conducive to the diffusion and dissolution of CO_2, too high CO_2 pressure will lead to the accumulation of $CaCO_2$ precipitation on the

sample surface, forming a passivation layer to block the pores and hinder the diffusion of CO_2 (Fig. 13b). However, according to the study of Boone et al., it is surprising that the compressive strength of steel slag compacts still rapidly enhances from 1.8 MPa to 52 MPa after 2 h mineralization with high CO_2 pressure (2 MPa)[86]. Therefore, under very high pressure of CO_2 , the effect of $CaCO_3$ passivation layer on the mineralization of steel slag compacts needs further analyses. It is worth noting that although increasing CO_2 pressure is beneficial to improve the performance of mineralized steel slag compacts, higher pressure means higher production costs. Moreover, the pressure and concentration of CO_2 in the flue gas is usually low. Direct utilization of flue gas contributes to saving the cost of CO_2 enrichment and concentration. Hence, from the perspective of large-scale application, the economic efficiency of high-pressure mineralization fails to satisfy the practical requirement. Generally, the common mineralization pressure of CO_2 is 0.05-1 MPa, making the mineralization reaction easy to control. Wang et al. proved that even if the steel slag bricks were mineralized for 24 h at a low pressure of 0.02 MPa, the mineralization efficiency still could reach 33.9% and presented available mechanical property[87].

In addition to temperature and CO_2 pressure, Humbert et al. investigated the effect of compacting pressure on mineralized steel slag compacts. The test results revealed that as the compacting pressure increased, the compacts porosity decreased, leading to higher compressive strength. However, when the compacting pressure further increased from 20 MPa to 30 MPa, the compressive strength only enhanced by 1.98%[27]. This suggests the existence of a critical compacting pressure. Zhang et al. obtained the similar results through response surface method that steel slag bricks exhibited maximum compressive strength at 8 MPa compacting pressure, with no significant improvement from higher pressures[88]. The phenomenon may be attributed to the fact that further increasing the compacting pressure excessively densifies the pores, thereby hindering CO_2 diffusion[89, 90]. Steel slag compacts with the highest density do not necessarily exhibit the highest compressive strength. In addition, different from the study of Humbert et al. and Zhang et al., Jiang et al. disclosed the negative correlation between compacting pressure and compressive strength when the w/b reached 0.18 [91] (Fig.13c). It was attributed to the fact that the improvement of compacting pressure promoted the pore water to act as lubricant, thus decreasing the compressive strength. Therefore, it is necessary to balance the relationship between compacting pressure, porosity, and w/b to determine the optimal compacting pressure, thus maximizing the compressive strength of mineralized steel slag compacts.

Besides confirming the effects of temperature and CO_2 pressure, Nielsen et al. also investigated the influence of moisture content on steel slag compacts[92]. The test results showed that steel slag compacts with 4% moisture content expressed lower CO_2 absorption compared to those with 10% moisture content. This is attributed to the fact that not all moisture in steel slag compacts is utilized for mineralization reaction. And some other processes involving evaporation, hydration, and silica gels absorption also consume moisture, resulting in insufficient residual moisture to support the mineralization reaction. However, the mineralization degree of steel slag compacts does not always correlate positively with moisture content. According to the studies of Wang et al., excessive moisture content in the pores of steel slag bricks blocked the path of CO_2 and reduced the mineralization degree[93]. The specific process is illustrated in Fig. 13d. Moreover, mineralization can be further enhanced by using more reasonable method to regulate moisture content. Shi et al. utilized ultraviolet light to reduce the moisture content of cement-fly ash compacts before mineralization, thus effectively improving the degree of mineralization and compressive strength[94]. Considering that moisture content is the key parameter of steel slag compacts during the mineralization, ultraviolet pretreatment provides a new strategy to accelerate mineralization.

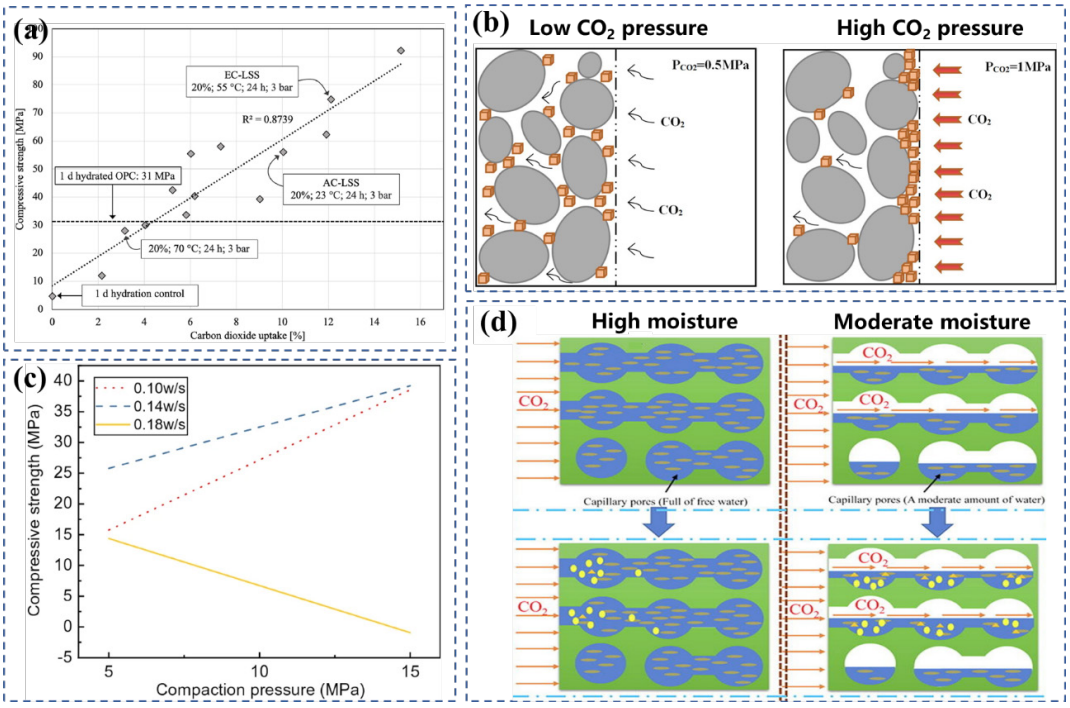

Fig. 13 Influence of mineralization condition: (a) temperature; (b) CO_2 pressure; (c) compacting pressure; (d) moisture content[85, 91, 93].

Table. 1 the strength under various mineralization conditions

Condition	Value	Compressive strength/ Mineralization efficiency	Reference
Temperature	23 °C	56.1 MPa	[80]
	55°C	74.7 MPa	
CO2 pressure	2 MPa	52 MPa	[86]
	0.02 MPa	33.9%	
Compacting pressure	10 MPa	45.6 MPa	[27]
	20 MPa	70.7 MPa	
	30 MPa	72.1 MPa	
	8 MPa	30 MPa	[88]
Moisture content	4%	60%	[92]
	10%	70%	

4.2.2. Material incorporation

When the performance of steel slag compacts cannot be further improved by optimizing the environment condition of mineralization, incorporating new materials with special properties may become a new strategy. For example, accelerating the diffusion of CO_2 in steel slag compacts is the key to further strengthen their mechanical performance and CO_2 sequestration. However, the balance between the compacting pressure and the porosity of the compact makes it difficult to improve pore connectivity while maintaining compactness. Therefore, an effective method is to introduce porous materials into dense compacts to improve the diffusion of CO_2. Biochar, as a typical porous material, is expected to provide diffusion channels for CO_2 without reducing the initial packing density. Zhang et al. disclosed the effect of biochar on the mineralization behaviors of steel slag compacts[95]. According to their results, the CO_2 uptake can increase to 15.6% at 5% biochar, and the mineralization depth can reach up to 10.1 mm at 10% biochar. The porous biochar structure creates more microchannels between steel slag particles, facilitating CO_2 diffusion and enhancing mineralization degree. It is noteworthy that both low and high dosage will lead to the decrease of CO_2 uptake and compressive strength in this work, but the reasons for the negative effect are different. As a highly porous material, biochar possesses strong water adsorption capacity,

which can reduce the content of available water, thus inhibiting the mineralization. When the dosage is too high (10%), biochar will weaken the mineralization due to the dilution of steel slag. Hence, utilizing materials with water-absorbing behavior to regulate mineralization need to carefully consider their dosage. Wang et al. investigated the mineralization behavior of steel slag compacts at various dosages of gypsum[96]. The CO_2 uptake of steel slag increases almost linearly with the addition of gypsum, indicating that gypsum effectively promotes the mineralization. This is because the addition of gypsum promotes the mineralization reactivity of mayenite (C12A7), accelerating the formation of monocarbonate. Moreover, Chang et al. utilized zeolite to further improve the properties of steel slag compacts[97, 98]. At the zeolite substitution ratios of 5 wt% and 15 wt%, the compressive strength and mineralization degree increase by 14% and 10.2%, respectively. The enhancement mechanism is mainly attributed to the fact that zeolite can react with CaO-FeO_X to generate additional C-S-H gel.

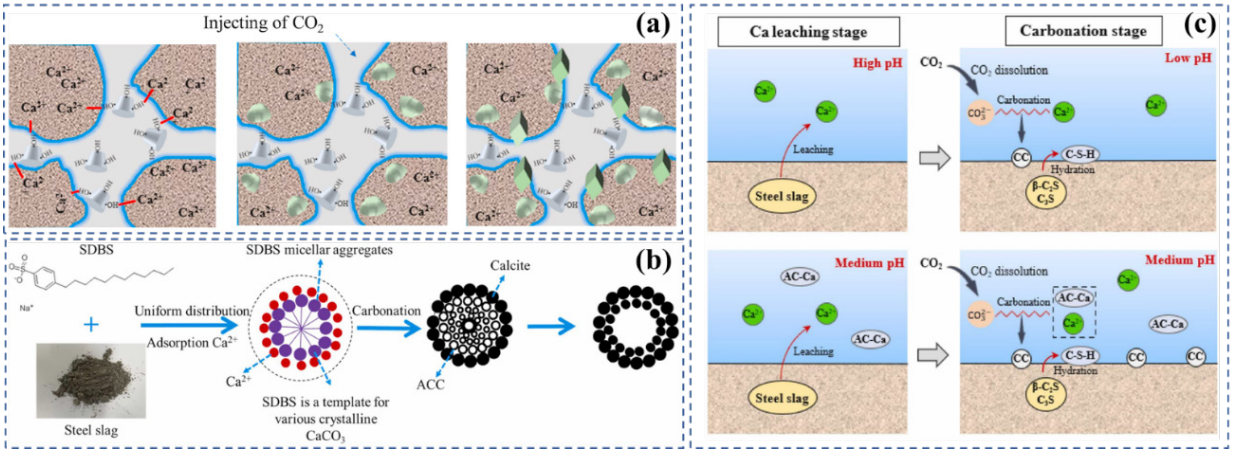

Fig. 14 Enhancement mechanism diagram of various additive: (a) β-CD; (b) SDBS; (c) AC[99-101].

Apart from adding solid materials, incorporating additives can also be employed to modify steel slag compacts. In the previous studies, β-Cyclodextrin (β-CD)[99], Sodium dodecyl benzene sulfonate (SDBS)[101], Ammonium Citrate (AC)[100], and glycine[102] have been proved to obviously enhance the mineralization of steel slag compacts. For example, the CO_2 uptake and compressive strength of steel slag compacts reached 17.9 % and 138.5 MPa at the optimal dosage of 2.5%, representing 21.8% and 13.4% improvement compared to those without β-CD[99]. Glycine could even increase compressive strength by 655% underwent 7 d mineralization[102]. The specific information is shown in Table 2. The common enhancement mechanisms of these additives above are mainly in the following aspects: 1) regulating the reaction process involving Ca^{2+} dissolution, nucleation energy and crystallization behavior to accelerate mineralization; 2) refining the mineralization products and filling the pore to densify the microstructure. Meanwhile, each additive also possesses special strengthening mechanism. Specifically, β-CD interacts with Ca^{2+} to form complexes to creates a supersaturated environment, reducing the activation energy for crystal nucleation and accelerating the mineralization (Fig. 14a); SDBS micelles can act as effective templates for the nucleation and growth of diverse $CaCO_3$ polymorphs, thereby modifying microstructure and enhancing the mechanical property of steel slag compacts (Fig. 14b); With respect to AC, it can promote the leaching of calcium before mineralization and the dissolution of CO_2 during the mineralization by regulating the pH value (Fig. 14c); In terms of glycine, it can stimulate the hydration of brownmillerite, thus forming various polymorphs of $CaCO_3$ and amorphous $Al(OH)_3$. In addition to making bricks, steel slag

powder also can be compacted into small cylinder as artificial steel slag aggregate (CSSA). Zhang et al. revealed that polycarboxylate superplasticizer (PCE) could effectively enhance the compressive strength of CSSA[103]. At the optimal dosage of 1%, the compressive strength achieves 164 MPa, marking a 141% improvement over CSSA without PCE. The enhancement mechanism is mainly attributed in two aspects: 1) the PCE molecules promote the leaching of Ca^{2+}; 2) the cross-linked PCE molecules by Ca^{2+} hinder the early mineralization reaction, conducing to CO_2 diffusion from outside to inside and producing a more homogeneous structure.

Table 2 Specifical information of steel slag compacts with various additive.

Additive	Binder	Optimal dosage	Mineralization time	Compressive strength	Improvement rate
β-CD	100% steel slag	2.5%	12 h	138 MPa	13.4%
AC	100% steel slag	0.1 mol/L	12 h	99.2 MPa	28.9%
SDBS	100% steel slag	0.2 mol/L	24 h	62.89 MPa	88.61%
glycine	100% steel slag	3 wt%	7 d	77.8 MPa	655%

Microbes and their enzymes play an extremely essential role in the natural environment. Various microbes can accomplish the interconversion between the CO_2 and $CaCO_3$[104, 105]. The application of microbes in cementitious is extremely innovative and promising due to their rapid reproduction, pollution-free, and high dispersion. Considering the complex composition of steel slag and the variations caused by different manufactured method, Jin et al. prepared the compacts of C_2S, the main component of steel slag, to investigate the effect of microbes on the mineralization of steel slag compacts[106]. The results showed that the compressive strength of C_2S compacts with microbes underwent 2 h mineralization reached over 75 MPa, nearly 30% higher than those without microbes. And microbes present positive effect on both the hydration and mineralization process of steel slag. Zhang et al. obtained the similar results utilizing Bacillus Mucilaginous and attributed the mechanism that microbes promoted mineralization and improved the properties of steel slag compacts to two aspects[107]: 1) Carbonic anhydrase secreted by microbes can effectively promote the dissolution process of CO_2 to generate HCO_3^- which is finally converted into CO_3^{2-}; 2) Carbonic can act as nucleation sites to adsorb silicate-leached Ca^{2+}, thereby accelerating the precipitation of mineralization products and filling the pore structure. Yi et al. and Jin et al. clearly described the nucleation sites effect of microbes and the pathway of microbial-secreted enzymes increased CO_3^{2-} concentration[108, 109], the detail was shown in Fig. 15. In addition to simplifying with single mineral phase, Qian et al. investigated the influence of microbes on steel slag bricks prepared using the casting method[110]. They discovered that bacterial powder had little effect on the strength of steel slag bricks that did not undergo mineralization. However, after mineralization, the compressive and flexural strengths of bricks with microbes were significantly higher compared to those without microbes. This also obviously suggests that microbes contribute to enhancing the mineralization process, hence improving the mechanical properties of steel slag bricks.

Although the microbe-induced modification is very significant, it is necessary to consider the effect of pH value on the microbial activity. For instance, the suitable pH value of Bacillus Mucilaginous is 8-11[111]. The activity of microbes and enzymes will decrease whether the pH value is too high or too low, thus weakening the modification effect. Generally, the pH value of steel slag paste will be higher than 12 before the mineralization, and then gradually decreases during the mineralization process[112, 113]. And microbes are usually added directly in the form of bacteria powder or dissolved in the mixing water. Therefore, microbes will undergo the high pH environment in the early age. The influence of pH value on the modification effectiveness of steel slag compacts needs to be further clarified in the follow-up exploration.

In conclusion, with the further investigation of steel slag mineralization, more and more enhancement strategies for steel slag compacts will be developed. However, steel slag compacts as building materials are large-scale use scenarios, the additional costs generated by extra treatment will be significantly amplified. Hence, it is essential to balance the performance improvement and the additional costs.

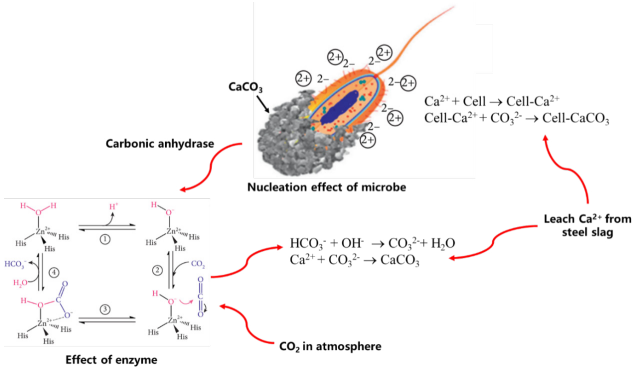

Fig. 15 Enhancement process involving nucleation effect and enzyme effect by microbe[108, 109].

5.Pilot tests and scale–up progress of mineralized steel slag products.

Owing to the property promotion of steel slag after carbon mineralization, the mineralized steel slag has shown the potential to be used as building materials, such as SCM, aggregate and steel slag blocks. To date, numerous researchers and enterprises have initiated pilot tests and scaled-up production of mineralized steel slag products. Mahoutian et al. presented a pilot study on a production of full-size mineralized steel slag masonry blocks and mineralized steel slag-bond concrete blocks, respectively[78, 114]. The experiment results demonstrated that two types of mineralized steel slag blocks exhibited equal or even better mechanical and durability properties compared to the commercial cement masonry block. The leaching properties and fire resistance performance of mineralized steel slag masonry blocks were satisfactory. In addition, they performed the economy analysis and carbon balance analysis of steel slag blocks as Table 3 and Table 4. The economy analysis showed the feasibility of making steel slag-bond concrete block with the lower price compared to the commercial cement block. Moreover, the production of mineralized steel slag-bond concrete block is environment friendly. The total CO_2 emitted for the commercial cement block was 1.56kg per 1 block produced. However, for mineralized steel slag-bond concrete block, the value was negative.

Table 3 Cost comparison between slag-bond concrete block and commercial cement block (US cents).

Id	Item	slag-bond concrete block (US cents/block)	Concrete masonry block (US cents/block)
(a)	Normal aggregate	0.0	20.9
(b)	Expanded aggregate	27.5	0.0
(c)	Steel slag	3.0	0.0
(d)	Cement	0.0	16.6
(e)	Transportation of cement	0.0	0.7
(f)	Transportation of aggregate	0.9	2.2
(g)	Transportation of slag	1.5	0.0
(h)	Grinding of steel slag	1.8	0.0
(i)	CO_2 capture and transportation	2.1	0.0
(j)	Steam curing	0.0	2.8
Total cost (US cents)		36.8	43.3

Table 4 Carbon balance analysis of producing slag and cement blocks.

Unit	Slag-bond concrete block				Cement block	
	Grinding steel slag	CO_2 removal and recovery	CO_2 compression and liquefaction	Slag uptake	Cement production	Steam curing
Energy (kWh/t)	36.7[a]	143.0[b]	103.0[b]	—	—	56kWh for 100 blocks
Energy for 1 block (kWh)	0.37	0.07	0.051	—	—	0.56
CO_2 emitted for 1 block(kg)	0.20	0.04	0.03	-0.50	1.26	0.30
Total CO_2 emitted for 1 block (kg)	-0.23				1.56	

a Calculated based on a 2.2 kW pulverizer run for 1 min to grind 1 kg of slag.

bHalmann, M.,Steinberg, M., 1999. Greenhouse gas carbon dioxide mitigation: Science and Technology, Lewis Publishers: Boca Raton, 568 pp.

Pilot tests have confirmed the feasibility of mineralized steel slag products. Current large-scale applications of carbon mineralization using steel slag primarily focus on producing calcium carbonate products, aiming to achieve both resource utilization of steel slag and carbon sequestration. In 2014, the Aalto

University constructed an indirect mineral carbonation pilot plant, which can produce about 10 kg of high-purity calcium carbonate by using 20 kg of steel slag [115]. Baotou Steel Group proposed the Carbonation Process Comprehensive Steel Slag Utilization Project. Its Phase I facility was officially commissioned in 2023, with an annual production capacity of 55,000 tons of high-purity filler-grade calcium-magnesium carbonate and 70,000 tons of green negative-carbon micro-powder. The project directly mineralizes 20,000 tons of CO_2 per year, achieving an overall annual carbon emission reduction of 120,000 tons. For the scale-up application of mineralized steel slag products, the key challenge lies in enhancing carbon mineralization rate and degree. Shi et al. firstly put forward the theory of "moisture regulation-gas migration-mineralization reaction" and developed the pre-curing technology, which significantly increased the carbon mineralization efficiency and made the large-scale production of carbon mineralization concrete products possible[2, 116]. In 2022, the research team led by Liu, in collaboration with Beijing Jingyun Taibo New Material Technology Co., Ltd., has established the world's first 10,000-ton-scale industrial pilot demonstration plant for direct CO_2 utilization. Their carbon mineralization technology enables the direct utilization of industrial exhaust gases with CO_2 concentrations as low as ≥10%. Each ton of carbon mineralization material can sequester 0.3–0.5 tons of carbon. In addition, Carbstone Innovation technology designed steel slag to sequestrate CO_2 and produce different low carbon materials including floor tiles, roofing tiles, clinkers and building blocks [117]. It uses 100% steel slags to form different shape with satisfied compressive strength and other properties.

6. Conclusions and prospects

This review comprehensively summarizes the mineralization behaviors and characteristics of steel slag, and analyzes the feasibility of large-scale application as building materials. The main conclusion and suggestion for future research are as follows:

(1) Mineralized steel slag compacts possess significant potential as building materials. The performance involving mechanical strength and durability is comparable or even better than those of cement-based products. In addition, it is necessary to balance the relationship between performance improvement and cost-efficiency in large-scale applications.

(2) Due to the poor stability of vaterite and aragonite, it is difficult to observe them in mineralized cementitious materials via conventional carbon mineralization conditions. Specific additives can increase the content of metastable $CaCO_3$, like ammonium salts and magnesium salts. Its effectiveness is influenced not only by the type and concentration of additives, and mineralization temperature, but also by the composition of the cementitious materials. With the incorporation of glycine, high purity vaterite can be produced via wet mineralization of carbide slag; whereas its polymorphic regulatory effect is very weak for steel slag.

(3) The mineralization models of steel slag are still in infancy stages. Moreover, compared to steel slag powder, the modeling process of steel slag compacts becomes more complex when considering the effects of multi-process coupling, numerous variables, and microstructure. In addition, due to variations in manufacturing processes, steel slag exhibits complex and diverse compositions. Investigations into steel slag-related models should not be confined to a single type of steel slag.

(4) Most existing studies of mineralized steel slag compacts primarily focus on testing their mechanical properties, with limited studies on their volume stability and freeze-thaw resistance. Future research requires prioritize long-term durability evaluations, as this is a fundamental prerequisite for the large-scale application of steel slag compacts as building materials.

(5) The forms of steel slag compacts mainly consist of bricks and slabs. Exploring more complex forms such as beams and columns would further broaden application scenarios.

Declaration of Competing Interest

There are no conflicts to declare.

Acknowledgements

The authors would like to acknowledge the financial support from National Natural Science Foundation of China grant numbers U22A20122, 52278257 and 52078204, and Innovandi core project 10 of Global Cement and Concrete Association (GCCA).

Reference

[1] C. Shi, Characteristics and cementitious properties of ladle slag fines from steel production, Cem. Concr. Res. 32 (2002) 459-462.

[2] S. Monkman, Y. Shao, C. Shi, Carbonated Ladle Slag Fines for Carbon Uptake and Sand Substitute, J. Mater. Civ. Eng. 21(11) (2009) 657-665.

[3] X. Liu, X. Liu, Z. Zhang, X. Ai, Effect of carbonation curing on the characterization and properties of steel slag-based cementitious materials, Cem. Concr. Compos. 154 (2024) 105769.

[4] U.S.G. Survey, Mineral commodity summaries, US geol. Surv (2021).

[5] R. Sun, P. Shen, D. Wang, J. Wang, Z. Liu, K. Fang, Enhancing hydration of steel slag-based composite cementitious material: Synergistic effect of triisopropanolamine (TIPA) and sulfite/sulfate, Cem. Concr. Res. 184 (2024) 107619.

[6] P. Liu, L. Mo, J. Zhong, M. Tang, In-situ investigation on the carbonation behaviors of various mineral phases in steel slag: The role of RO phase, Cem. Concr. Compos. 149 (2024) 105524.

[7] H. Yi, G. Xu, H. Cheng, J. Wang, Y. Wan, H. Chen, An Overview of Utilization of Steel Slag, Procedia Environ. Sci. 16 (2012) 791-801.

[8] C. Shi, J. Qian, High performance cementing materials from industrial slags — a review, Resour. Conserv. Recycl. 29 (2000) 195-207.

[9] J. Liu, C. Zeng, Z. Li, G. Liu, W. Zhang, G. Xie, F. Xing, Carbonation of steel slag at low CO_2 concentrations: Novel biochar cold-bonded steel slag artificial aggregates, Sci. Total Environ. 902 (2023) 166065.

[10] J. O'Connor, T.B.T. Nguyen, T. Honeyands, B. Monaghan, D. O'Dea, J. Rinklebe, A. Vinu, S.A. Hoang, G. Singh, M.B. Kirkham, N. Bolan, Production, characterisation, utilisation, and beneficial soil application of steel slag: A review, J. Hazard. Mater. 419 (2021) 126478.

[11] X. Chen, X. Sun, P. Xu, S. Wang, T. Zhou, X. Wang, C. Yang, Q. Lu, Optimal regulation of N/P in horizontal sub-surface flow constructed wetland through quantitative phosphorus removal by steel slag fed, Environ. Sci. Pollut. Res. 27(6) (2019) 5779-5787.

[12] Q. Dong, G. Wang, X. Chen, J. Tan, X. Gu, Recycling of steel slag aggregate in portland cement concrete: An overview, J. Cleaner Prod. 282 (2021) 124447.

[13] P.S. Humbert, J. Castro-Gomes, CO_2 activated steel slag-based materials: A review, J. Cleaner Prod. 208 (2019) 448-457.

[14] X. Hu, P. He, C. Shi, Carbonate binders: Historic developments and perspectives, Cem. Concr. Res. 175 (2024) 107352.

[15] Z. Chen, R. Li, J. Liu, Preparation and properties of carbonated steel slag used in cement cementitious materials, Constr. Build. Mater. 283 (2021) 122667.

[16] C. Shi, Steel Slag—Its Production, Processing, Characteristics, and Cementitious Properties, J. Mater. Civ. Eng 16((3)) (2004) 230-236.

[17] Y. Wang, J. Liu, X. Hu, J. Chang, T. Zhang, C. Shi, Utilization of accelerated carbonation to enhance the application of steel slag: a review, J. Sustainable Cem.-Based Mater. 12(4) (2022) 471-486.

[18] W. Li, M. Cao, D. Wang, J. Zhao, J. Chang, Improving the hydration activity and volume stability of the RO phases in steel slag by combining alkali and wet carbonation treatments, Cem. Concr. Res. 172 (2023) 107236.

[19] X. Zhu, H. Hou, X. Huang, M. Zhou, W. Wang, Enhance hydration properties of steel slag using grinding aids by mechanochemical effect, Constr. Build. Mater. 29 (2012) 476-481.

[20] S.K. Singh, Jyoti, P. Vashistha, Development of newer composite cement through mechano-

chemical activation of steel slag, Constr. Build. Mater. 268 (2021) 121147.
[21] D. Fan, C. Zhang, J.-X. Lu, K. Liu, T. Yin, E. Dong, R. Yu, Recycling of steel slag powder in green ultra-high strength concrete (UHSC) mortar at various curing conditions, J. Build. Eng. 70 (2023) 106361.
[22] C. Shi, F. He, Y. Wu, Effect of pre-conditioning on CO_2 curing of lightweight concrete blocks mixtures, Constr. Build. Mater. 26(1) (2012) 257-267.
[23] B. Lu, C. Shi, G. Hou, Strength and microstructure of CO_2 cured low-calcium clinker, Constr. Build. Mater. 188 (2018) 417-423.
[24] B. Lu, C. Shi, Z. Cao, M. Guo, J. Zheng, Effect of carbonated coarse recycled concrete aggregate on the properties and microstructure of recycled concrete, J. Cleaner Prod. 233 (2019) 421-428.
[25] J. Chang, Y. Fang, X. Shang, The role of β-C2S and γ-C2S in carbon capture and strength development, Mater. Struct. 49(10) (2016) 4417-4424.
[26] X. Xian, M. Mahoutian, D. Zhang, Y. Shao, Development of wet-cast Portland-cement-free concrete based on steel slag and ambient-pressure carbonation activation, Resour. Conserv. Recycl. 203 (2024) 107455.
[27] P.S. Humbert, J.P. Castro-Gomes, H. Savastano, Clinker-free CO_2 cured steel slag based binder: Optimal conditions and potential applications, Constr. Build. Mater. 210 (2019) 413-421.
[28] Z. Ghouleh, R.I.L. Guthrie, Y. Shao, High-strength KOBM steel slag binder activated by carbonation, Constr. Build. Mater. 99 (2015) 175-183.
[29] Q. Zhang, P. Feng, X. Shen, Y. Cai, H. Zhen, Z. Liu, Comparative analysis of carbonation strengthening mechanisms in full solid waste materials: Steel slag vs. carbide slag, Cem. Concr. Compos. 157 (2025) 105927.
[30] I.Z. Yildirim, M. Prezzi, Chemical, Mineralogical, and Morphological Properties of Steel Slag, Adv. Civ. Eng. 2011 (2011) 1-13.
[31] J. Setién, D. Hernández, J.J. González, Characterization of ladle furnace basic slag for use as a construction material, Constr. Build. Mater. 23(5) (2009) 1788-1794.
[32] P. Liu, J. Zhong, M. Zhang, L. Mo, M. Deng, Effect of CO_2 treatment on the microstructure and properties of steel slag supplementary cementitous materials, Constr. Build. Mater. 309 (2021) 125171.
[33] C. Shi, S. Hu, Cementitious properties of ladle slag fines under autoclave curing conditions, Cem. Concr. Res. 33(11) (2003) 1851-1856.
[34] J.M. Bukowski, R.L. Berger, Reactivity and strength development of CO_2 activated non-hydraulic calcium silicates, Cem. Concr. Res. 9 (1979) 57-68.
[35] L. Mo, F. Zhang, M. Deng, Mechanical performance and microstructure of the calcium carbonate binders produced by carbonating steel slag paste under CO_2 curing, Cem. Concr. Res. 88 (2016) 217-226.
[36] S. Zhang, Z. Ghouleh, A. Mucci, O. Bahn, R. Provençal, Y. Shao, Production of cleaner high-strength cementing material using steel slag under elevated-temperature carbonation, J. Cleaner Prod. 342 (2022) 130948.
[37] J. Chen, Y. Xing, Y. Wang, W. Zhang, Z. Guo, W. Su, Application of iron and steel slags in mitigating greenhouse gas emissions: A review, Sci. Total Environ. 844 (2022) 157041.
[38] Z. Zhang, K. Zheng, L. Chen, Q. Yuan, Review on accelerated carbonation of calcium-bearing minerals: Carbonation behaviors, reaction kinetics, and carbonation efficiency improvement, J. Build. Eng. 86 (2024) 108826.
[39] X. Huang, J. Zhang, L. Zhang, Accelerated carbonation of steel slag: A review of methods, mechanisms and influencing factors, Constr. Build. Mater. 411 (2024) 134603.
[40] L. Li, T. Chen, M. Sun, X. Gao, X. He, G. Geng, 3D nanostructure of CO_2□mineralized steel slag, J. Am. Ceram. Soc. 108(4) (2024).
[41] J. Chang, D. Wang, Y. Fang, Effects of mineralogical changes in BOFS during carbonation on pH and Ca and Si leaching, Constr. Build. Mater. 192 (2018) 584-592.
[42] Y. Li, H. Liao, Y. Guo, Aqueous carbonation of steel slag and preparation of calcium carbon: A

new strategy for the utilization of steel slag, J. Environ. Chem. Eng. 13(2) (2025).
[43] S.N. Lekakh, C.H. Rawlins, D.G.C. Robertson, V.L. Richards, K.D. Peaslee, Kinetics of Aqueous Leaching and Carbonization of Steelmaking Slag, Metallurgical and Materials Transactions B 39B (2008) 125-134.
[44] Z.X. Chen, N.T. Zhang, S.H. Chu, Role of alkalinity in CO_2 sequestration of γ-belite, Constr. Build. Mater. 432 (2024) 136508.
[45] S. Lin, P. Chen, W. Xiang, C. Hu, F. Li, J. Liu, Y. Ding, Exploring the Effect of Moisture on CO_2 Diffusion and Particle Cementation in Carbonated Steel Slag, Applied Sciences 14(3631) (2024) 1-15.
[46] Z. Luo, Y. Wang, G. Yang, J. Ye, W. Zhang, Z. Liu, Y. Mu, Effect of curing temperature on carbonation behavior of steel slag compacts, Constr. Build. Mater. 291 (2021) 123369.
[47] S. Tian, J. Jiang, X. Chen, F. Yan, K. Li, Direct Gas–Solid Carbonation Kinetics of Steel Slag and the Contribution to In situ Sequestration of Flue Gas CO_2 in Steel□Making Plants, ChemSusChem 6 (2013) 2348-2355.
[48] Huijgen, W.J. J, Witkamp, Geert-Jan, Comans, R.N. J, Mineral CO_2 sequestration by steel slag carbonation, Environ. Sci. Technol. 39 (2005) 9676-9682.
[49] M. Spanka, T. Mansfeldt, R. Bialucha, Influence of Natural and Accelerated Carbonation of Steel Slags on Their Leaching Behavior, Steel Research International 87 (2016) 798-809.
[50] P. Librandi, P. Nielsen, G. Costa, R. Snellings, M. Quaghebeur, R. Baciocchi, Mechanical and environmental properties of carbonated steel slag compacts as a function of mineralogy and CO_2 uptake, J. CO_2 Util. 33 (2019) 201-214.
[51] M. Tu, H. Zhao, Z. Lei, L. Wang, D. Chen, H. Yu, T. Qi, Aqueous Carbonation of Steel Slag: A Kinetics Study, ISIJ Int. 55(11) (2015) 2509-2514.
[52] J. Kim, G. Azimi, The CO_2 sequestration by supercritical carbonation of electric arc furnace slag, J. CO_2 Util. 52 (2021) 101667.
[53] C. DiGiovanni, O.A. Hisseine, A.N. Awolayo, Carbon dioxide sequestration through steel slag carbonation: Review of mechanisms, process parameters, and cleaner upcycling pathways, J. CO_2 Util. 81 (2024) 102736.
[54] Z. Wang, S. Xu, S. Zheng, H. Duan, D. Chen, M. Long, Y. Li, Accelerated carbonation and stabilization of BOF slag: data fitting relationship between particle size and CO_2 sequestration, J. Sustainable Cem.-Based Mater. 13(5) (2024) 726-737.
[55] S.-M. Shih, C.u.-S. Ho, Y.-S. Song, J.-P. Lin, Kinetics of the Reaction of Ca(OH)2 with CO_2 at Low Temperature, Industrial & Engineering Chemistry Research 38 (1999) 1316-1322.
[56] S.-Y. Pan, P.-C. Chiang, Y.-H. Chen, C.-S. Tan, E.E. Chang, Kinetics of carbonation reaction of basic oxygen furnace slags in a rotating packed bed using the surface coverage model: Maximization of carbonation conversion, Appl. Energy 113 (2014) 267-276.
[57] N. Zhang, G. Deng, W. Liao, H. Ma, C. Hu, Aqueous carbonation of steel slags: A comparative study on mechanisms, Cem. Concr. Compos. 155 (2025) 105838.
[58] Y. Tan, Z. Liu, F. Wang, Effect of temperature on the carbonation behavior of γ-C2S compacts, Cem. Concr. Compos. 133 (2022) 104652.
[59] J. Chang, H. Wu, Study on carbonation mechanism of steel slag, journal of the Chinese ceramic society 38(7) (2010) 1186-1190.
[60] S. Yadav, A. Mehra, Experimental study of dissolution of minerals and CO_2 sequestration in steel slag, Waste Manage. (Oxford) 64 (2017) 348-357.
[61] X. Wang, X. Wei, W. Ni, Impacts of hydration degree of steel slag on its subsequent CO_2 capture behaviors and mechanical performances of prepared building materials, Constr. Build. Mater. 416 (2024) 135075.
[62] Y. Fang, J. Shan, Q. Wang, M. Zhao, X. Sun, Semi-dry and aqueous carbonation of steel slag: Characteristics and properties of steel slag as supplementary cementitious materials, Constr. Build. Mater. 425 (2024) 135981.
[63] X. Liu, P. Wu, X. Liu, Z. Zhang, X. Ai, The Utilization of Carbonated Steel Slag as a Supplementary Cementitious Material in

Cement, Materials 17(4574) (2024) 1-26.
[64] D. Zhao, J.M. Williams, P. Hou, A.J. Moment, S. Kawashima, Stabilizing mechanisms of metastable vaterite in cement systems, Cem. Concr. Res. 178 (2024) 107441.
[65] P. Shen, J. Lu, Y. Zhang, Y. Jiang, S. Zhang, C.S. Poon, Preparation aragonite whisker-rich materials by wet carbonation of cement: Towards yielding micro-fiber reinforced cement and sequestrating CO_2, Cem. Concr. Res. 159 (2022) 106891.
[66] Y.-J. Wang, J.-G. Li, M.-J. Tao, X. Zhang, J.-B. Zhang, S. Qin, S.-H. Liu, L.-J. Peng, X.-P. Zhang, Y.-N. Zeng, Investigation of the acicular aragonite growth behavior in AOD stainless steel slag during slurry-phase carbonation, Sci. Total Environ. 904 (2023) 166750.
[67] J.M. Williams, D. Zhao, N. Zhang, A. Chin, S. Kawashima, A.J. Moment, Directed synthesis of aragonite through semi-continuous seeded crystallization methods for CO_2 utilization, CrystEngComm 25 (2023) 6050-6066.
[68] Q. Zhou, A. Meawad, W. Wang, T. Noguchi, Stabilization of metastable calcium carbonate polymorphs on the surface of recycled cement paste particles: A two-step carbonation approach without chemical additives, Cem. Concr. Compos. 155 (2025) 105829.
[69] X. Ding, W. Li, J. Chang, Preparation of aragonite from calcium carbonate via wet carbonation to improve properties of steel slag building materials, Constr. Build. Mater. 451 (2024) 138763.
[70] Y. Xue, T. Chen, X. Zhao, J. Liu, Effect of acidic amino acids on wet pre-carbonation of β-C2S in steel slag, Mater. Today Commun. 35 (2023) 105835.
[71] X. Song, Y. Tuo, Y. Liang, Z. Tang, M. Li, X. Hua, R. Yang, X. Bu, X. Luo, Effects of NH4+ concentration on the vaterite formation via direct carbonation use waste carbide slag under the different ammonium systems, J. Environ. Chem. Eng. 11 (2023) 111583.
[72] Y. Zhou, F. Wu, L. Jinag, B. Lu, G. Hou, J. Zhu, Production of vaterite via wet carbonation of carbide residue: Enhancing cement properties and CO_2 sequestration, Cem. Concr. Compos. 150 (2024) 105549.
[73] P. Cao, X. Zhao, Y. Wang, Z. Zhang, J. Liu, Effect of Glycine on the Wet Carbonation of Steel Slag Used as a Cementitious Material, Materials 17(451) (2024) 1-16.
[74] L. Mo, F. Zhang, M. Deng, F. Jin, A. Al-Tabbaa, A. Wang, Accelerated carbonation and performance of concrete made with steel slag as binding materials and aggregates, Cem. Concr. Compos. 83 (2017) 138-145.
[75] G. Hou, Z. Yan, J. Sun, H.M. Naguib, B. Lu, Z. Zhang, Microstructure and mechanical properties of CO_2-cured steel slag brick in pilot-scale, Constr. Build. Mater. 271 (2021) 121581.
[76] B. Pang, Z. Zhou, H. Xu, Utilization of carbonated and granulated steel slag aggregate in concrete, Constr. Build. Mater. 84 (2015) 454-467.
[77] Q. Wang, D. Wang, S. Zhuang, The soundness of steel slag with different free CaO and MgO contents, Constr. Build. Mater. 151 (2017) 138-146.
[78] M. Mahoutian, Y. Shao, Production of cement-free construction blocks from industry wastes, J. Cleaner Prod. 137 (2016) 1339-1346.
[79] X. Xian, M. Mahoutian, D. Zhang, Y. Shao, Z. Yu, Carbon capture and utilization using cement-free concrete products via near-ambient pressure carbonation, Int. J. Greenhouse Gas Control 134 (2024) 104130.
[80] S. Zhang, Z. Ghouleh, J. Liu, Y. Shao, Converting ladle slag into high-strength cementing material by flue gas carbonation at different temperatures, Resour. Conserv. Recycl. 174 (2021) 105819.
[81] Z. Ghouleh, R.I.L. Guthrie, Y. Shao, Production of carbonate aggregates using steel slag and carbon dioxide for carbon-negative concrete, J. CO_2 Util. 18 (2017) 125-138.
[82] B. Lu, S. Drissi, J. Liu, X. Hu, B. Song, C. Shi, Effect of temperature on CO_2 curing, compressive strength and microstructure of cement paste, Cem. Concr. Res. 157 (2022) 106827.
[83] E. Drouet, S. Poyet, P. Le Bescop, J.-M.

Torrenti, X. Bourbon, Carbonation of hardened cement pastes: Influence of temperature, Cem. Concr. Res. 115 (2019) 445-459.
[84] X. Zhang, J. Zhao, Y. Liu, J. Li, Use of steel slag as carbonation material: A review of carbonation methods and evaluation, environmental factors and carbon conversion process, J. CO_2 Util. 88 (2024) 102947.
[85] X. Zhong, L. Li, Y. Jiang, T.-C. Ling, Elucidating the dominant and interaction effects of temperature, CO_2 pressure and carbonation time in carbonating steel slag blocks, Constr. Build. Mater. 302 (2021) 124158.
[86] M.A. Boone, P. Nielsen, T. De Kock, M.N. Boone, M. Quaghebeur, V. Cnudde, Monitoring of Stainless-Steel Slag Carbonation Using X-ray Computed Microtomography, Environ. Sci. Technol. 48(1) (2013) 674-680.
[87] D. Wang, H. Zhang, M. Liu, Y. Fu, Z. Si, X. Zhang, Q. Zhong, The characterization and mechanism of carbonated steel slag and its products under low CO_2 pressure, Mater. Today Commun. 35 (2023) 105827.
[88] X. Zhang, D. Zhang, P. Wang, J. Deng, L. Gu, H. Yuan, Optimizing the properties of carbonated steel slag brick based on response surface method (RSM), Constr. Build. Mater. 473 (2025) 140921.
[89] M. Quaghebeur, P. Nielsen, L. Horckmans, D. Van Mechelen, Accelerated Carbonation of Steel Slag Compacts: Development of High-Strength Construction Materials, Front. Energy Res. 3 (2015).
[90] Y. Fang, J. Chang, M. Cao, Influence of compaction pressure on the accelerated carbonation of calcium hydroxide, Journal of Wuhan University of Technology-Mater. Sci. Ed. 31(6) (2016) 1187-1192.
[91] Y. Jiang, T.-C. Ling, Interdependent factors contributing towards carbonation of steel slag compact: consideration of casting pressure, water dosage and carbonation duration, Mater. Struct. 54(4) (2021) 176.
[92] P. Nielsen, M.A. Boone, L. Horckmans, R. Snellings, M. Quaghebeur, Accelerated carbonation of steel slag monoliths at low CO_2 pressure – microstructure and strength development, J. CO2 Util. 36 (2020) 124-134.
[93] R. Wang, P. Jin, H. Dong, Y. Liu, Z. Ding, W. Zhang, Effect of moist content on the bio-carbonated steel slag bricks, Constr. Build. Mater. 269 (2021) 121313.
[94] X.-C. Shi, Z. Shui, X. Xiao, Use of ultraviolet pretreatment to enhance carbonation properties of fly-ash cement under accelerated carbonation at different CO2 concentrations, J. Build. Eng. 75 (2023) 106983.
[95] T. Zhang, L. Wang, W. Zhu, Y. Guo, Z. Chen, J. Li, J. Wei, Q. Yu, Preparation of high strength carbon negative building material by CO2 curing biochar- EAF steel slag compacts, Constr. Build. Mater. 441 (2024) 137456.
[96] X. Wang, W. Ni, J. Li, S. Zhang, M. Hitch, R. Pascual, Carbonation of steel slag and gypsum for building materials and associated reaction mechanisms, Cem. Concr. Res. 125 (2019) 105893.
[97] J. Chang, X. Zhang, Y.y. Gu, Y.y. Zhang, Effects of pozzolanic reaction on carbonation degree and strength of steel slag compacts containing zeolite, Constr. Build. Mater. 277 (2021) 122334.
[98] X. Zhang, B. Wang, J. Chang, Effect of zeolite calcination temperature on the carbonation degree and strength of steel slag compacts, Constr. Build. Mater. 343 (2022) 127987.
[99] J. Huang, Y. Li, Y. Zhang, Enhancing effect of β-cyclodextrin on carbonation properties of steel slag, J. Build. Eng. 97 (2024) 110805.
[100] Z. Chen, Y. Liu, B. He, X. Jing, D. Cang, L. Zhang, Role of ammonium citrate in the preparation of high-strength carbonated steel slag cementitious materials, Constr. Build. Mater. 422 (2024) 135612.
[101] Y. Zhang, G. Li, S. Zhang, S. Luo, X. Guan, J. Zhu, X. Zhou, S. Liu, Enhancing mechanical properties of carbonated steel slag through surfactant-assisted CaCO3 crystallization, Constr. Build. Mater. 451 (2024) 138800.
[102] S. Kim, J. Kim, D. Jeon, J. Yang, J. Moon, Enhanced mechanical property of steel slag through glycine-assisted hydration and

carbonation curing, Cem. Concr. Compos. 149 (2024) 105532.
[103] Y. Zhang, M. Zhang, D. Huang, Polycarboxylate superplasticizer as strengthening additive in carbonated artificial steel slag aggregate, Constr. Build. Mater. 403 (2023) 133136.
[104] M. Kanwal, R.A. Khushnood, W. Khaliq, A.G. Wattoo, T. Shahid, Synthesis of pyrolytic carbonized bagasse to immobilize Bacillus subtilis; application in healing micro-cracks and fracture properties of concrete, Cem. Concr. Compos. 126 (2022) 104334.
[105] S. Xia, W. Song, Controls on microbially-induced carbonate precipitation in geologic porous media, Sci. Total Environ. 957 (2024) 177647.
[106] P. Jin, R. Wang, Y. Su, H. Dong, Q. Wang, Study on carbonation process of β-C2S under microbial enzymatic action, Constr. Build. Mater. 228 (2019) 117110.
[107] X. Zhang, C. Qian, H. Yi, Z. Ma, Study on carbonation reactivity of silicates in steel slag accelerated by Bacillus mucilaginosus, Constr. Build. Mater. 292 (2021) 123433.
[108] H. Yi, C.-x. Qian, Z. Luo, The Influence of Microbial Agent on the Mineralization Rate of Steel Slag, Adv. Mater. Sci. Eng. 2018(1) (2018).
[109] Peng Jin, Siyi Zhang, Yu Liu, Wei Zhang, Ruixing Wang, Application of Bacillus mucilaginosus in the carbonation of steel slag, Appl. Microbiol. Biotechnol. 105 (2021) 8663-8674.
[110] K. Wang, C. Qian, R. Wang, The properties and mechanism of microbial mineralized steel slag bricks, Constr. Build. Mater. 113 (2016) 815-823.
[111] C. Qian, X. Yu, T. Zheng, Y. Chen, Review on bacteria fixing CO2 and bio-mineralization to enhance the performance of construction materials, J. CO2 Util. 55 (2022) 101849.
[112] S. Yang, L. Mo, D. Lu, Effects of sodium aluminate on fleeting semi-dry carbonation and properties of steel slag powders in low concentration CO2 atmosphere, Cem. Concr. Compos. 150 (2024) 105551.
[113] J. Zhao, Z. Li, D. Wang, P. Yan, L. Luo, H. Zhang, H. Zhang, X. Gu, Hydration superposition effect and mechanism of steel slag powder and granulated blast furnace slag powder, Constr. Build. Mater. 366 (2023) 130101.
[114] M. Mahoutian, O. Chaallal, Y. Shao, Pilot production of steel slag masonry blocks, Can. J. Civ. Eng. (2018) 2-34.
[115] A. Said, T. Laukkanen, M. Järvinen, Pilot-scale experimental work on carbon dioxide sequestration using steelmaking slag, Appl. Energy 177 (2016) 602-611.
[116] C. Shi, Y. Wu, Studies on some factors affecting CO2 curing of lightweight concrete products, Resour. Conserv. Recycl. 52(8-9) (2008) 1087-1092.
[117] J. Mertens, C. Breyer, K. Arning, A. Bardow, R. Belmans, A. Dibenedetto, S. Erkman, J. Gripekoven, G. Léonard, S. Nizou, D. Pant, A.S. Reis-Machado, P. Styring, J. Vente, M. Webber, C.J. Sapart, Carbon capture and utilization: More than hiding CO2 for some time, Joule 7(3) (2023) 442-449.